Cellular Physiology and Biochemistry

Cell Physiol Biochem 2018;48:2011-2034
DOI: 10.1159/000492523
Published online: August 9, 2018
Accepted: July 30, 2018

Original Paper

Disassembly of Subplasmalemmal Actin Filaments Induces Cytosolic Ca^{2+} Increases in *Astropecten aranciacus* Eggs

Filip Vasilev[a] Nunzia Limatola[a] Dae-Ryoung Park[b] Uh-Hyun Kim[b] Luigia Santella[a] Jong Tai Chun[a]

[a]Department of Biology and Evolution of Marine Organisms, Stazione Zoologica Anton Dohrn, Napoli, Italy, [b]Chonbuk National University, Jeon Ju, Korea

Key Words
Actin • Calcium • Fertilization • Phospholipase C • Inositol trisphosphate • Latrunculin

Abstract
Background/Aims: Eggs of all animal species display intense cytoplasmic Ca^{2+} increases at fertilization. Previously, we reported that unfertilized eggs of *Astropecten aranciacus* exposed to an actin drug latrunculin A (LAT-A) exhibit similar Ca^{2+} waves and cortical flashes after 5-10 min time lag. Here, we have explored the molecular mechanisms underlying this unique phenomenon. ***Methods:*** Starfish eggs were pretreated with various agents such as other actin drugs or inhibitors of phospholipase C (PLC), and the changes of the intracellular Ca^{2+} levels were monitored by use of Calcium Green in the presence or absence of LAT-A. The concomitant changes of the actin cytoskeleton were visualized with fluorescent F-actin probes in confocal microscopy. ***Results:*** We have shown that the LAT-A-induced Ca^{2+} increases are related to the disassembly of actin filaments: *i)* not only LAT-A but also other agents depolymerizing F-actin (i.e. cytochalasin B and mycalolide B) induced similar Ca^{2+} increases, albeit with slightly lower efficiency; *ii)* drugs stabilizing F-actin (i.e. phalloidin and jasplakinolide) either blocked or significantly delayed the LAT-A-induced Ca^{2+} increases. Further studies utilizing pharmacological inhibitors of PLC (U-73122 and neomycin), dominant negative mutant of PLC-ɣ, specific sequestration of PIP2 (RFP-PH), $InsP_3$ uncaging, and quantitation of endogenous $InsP_3$ all indicated that LAT-A induces Ca^{2+} increases by stimulating PLC rather than sensitizing $InsP_3$ receptors. In support of the idea, it bears emphasis that LAT-A timely increased intracellular contents of $InsP_3$ with concomitant decrease of PIP2 levels in the plasma membrane. ***Conclusion:*** Taken together, our results suggest that suboolemmal actin filaments may serve as a scaffold for cell signaling and modulate the activity of the key enzyme involved in intracellular Ca^{2+} signaling.

Jong Tai Chun, Ph.D
and Prof. Kim Uh-Hyun

Biology and Evolution of Marine Organisms, Stazione Zoologica Anton Dohrn
Villa Comunale 1, Napoli, 80121 (Italy)
Tel. +39-081-583-3407, Fax +39-081-583-3289, E-Mail chun@szn.it; uhkim@chonbuk.ac.kr

Introduction

Owing to the large cell size and other unique characters, oocytes and eggs have been utilized for a variety of biological researches on a single cell basis [1]. Like nerve and muscle cells, oocytes and eggs are electrically excitable, as their plasma membrane is studded with various voltage-sensitive ion channels [2]. In addition, their cytoplasm comprises an excitable matrix that can propagate intracellular Ca^{2+} waves by mobilizing the internal stores such as endoplasmic reticulum (ER). This is due to the concerted actions of intracellular ion channels on the Ca^{2+} store that respond to Ca^{2+}-releasing second messengers such as inositol 1,4,5-trisphosphate ($InsP_3$), cyclic ADP-ribose (cADPr), and nicotinic acid adenine dinucleotide (NAADP) [3-6]. Thus, occurrence of active ion fluxes across the intracellular and plasma membranes during physiological processes is one of the characteristic features of oocytes and eggs. Indeed, the first visual demonstration of intracellular Ca^{2+} waves was made with the fertilized eggs of fish and echinoderms by use of Ca^{2+}-sensitive fluorescent probes [7, 8]. Fertilized eggs of all animal species manifest a massive increase of intracellular Ca^{2+} mainly in two modes, i.e. influx from the extracellular media and the ligand-gated release from the intracellular stores, and the Ca^{2+} signals play important roles in the resumption of cell cycle and the subsequent embryonic development [5, 6, 9-13].

When fertilized, echinoderm eggs loaded with calcium dye readily display a rapid, but short-lived, synchronized increase of Ca^{2+} underneath the entire plasma membrane. This Ca^{2+} signal is called 'cortical flash' and is known to be linked to swift depolarization of the membrane potential and the opening of L-type Ca^{2+} channels [14-16]. Cortical flash alone, however, is not sufficient to activate eggs at fertilization, and requires a prolonged and more intense Ca^{2+} response that starts at the sperm interaction site and propagates to the antipode. This Ca^{2+} wave is accompanied by a contraction wave and exocytosis of cortical granules. The extruded contents of cortical granules are thus deposited outside the plasma membrane, which elevates the vitelline layer and form fertilization envelope to protect the embryo. Furthermore, the Ca^{2+} wave in the fertilized eggs triggers a series of biochemical and cytological changes that are collectively termed 'egg activation' [13, 17-19].

While the crucial roles played by Ca^{2+} in egg activation were demonstrated by use of calcium ionophores or chelators [20, 21], the precise mechanisms by which the successful sperm triggers the Ca^{2+} wave in fertilized eggs have not been fully understood and may substantially differ from species to species. Among several hypotheses set forth, the 'receptor model' suggests a biochemical pathway involving a signal-transducing receptor on the egg surface, whereas the 'soluble sperm factor model' proposes sperm-borne signaling substances diffusing into the egg to evoke a Ca^{2+} increase. Nonetheless, the common denominator of the two models is the *de novo* synthesis or increment of the aforementioned Ca^{2+}-releasing second messengers, e.g. $InsP_3$, cADPr, and NAADP, at the end of the signaling cascade, which bind to their cognate ligand-gated ion channels on the Ca^{2+} stores [5, 22]. However, the contribution made by each second messenger may be quite different depending on the animal species. For example, whereas cADPr may provide an alternative path to generate the Ca^{2+} wave in fertilized eggs of sea urchin, its contribution in the fertilized eggs of certain species of starfish (e.g. *Asterina pectinifera*) appears to be negligible. Furthermore, while NAADP evokes a strong Ca^{2+} response in *A. pectinifera*, its effect inside the eggs of another species of starfish (e.g. *Astropecten aranciacus*) is remarkably weaker [23-27]. On the other hand, the seemingly universal pathway involving $InsP_3$ as the second messenger may have diverse modes of generating Ca^{2+} waves in the fertilized eggs of different animal species [28]. This is because the enzyme that synthesizes $InsP_3$ and diacylglycerol from phosphatidylinositol 4,5-bisphosphate (PIP2) exists in multiple isoforms [22, 29, 30]. In mammalian eggs, for example, a sperm-specific isoform PLCζ is accountable for generating Ca^{2+} waves at fertilization [31, 32]. PLCζ, however, does not seem to exist in the genome or transcriptome of sea urchin and starfish [33-35], and the $InsP_3$-dependent Ca^{2+} increase in the fertilized eggs of echinoderms is mostly attributable to PLCγ [36-38], which is shown to be activated by Src-family kinase that interacts with the SH domain of PLCγ within 15 sec after

fertilization [39-41]. Even so, questions still remain on how Src-family kinases are activated by their upstream signaling molecules on the egg surface. On the other hand, circumstantial evidence from experiments utilizing metabolically stable GTP and GDP suggested that Ca^{2+} signaling in fertilized sea urchin eggs might also involve PLCß, the isozyme activated by heterotrimeric G-protein. However, in light of the fact that GTP/GDP could interfere with many other G-proteins, interpretation of the data based on guanidine nucleotides alone had to be compromised [28, 42-44]. Hence, the origin of the sperm-induced Ca^{2+} signals in fertilized eggs of echinoderms is still obscure.

Cell signaling at fertilization inevitably directs our attention to the outermost region of egg cytoplasm, which is often referred to as 'ectoplasm' [45]. This subplasmalemmal region is crowded with meshwork of actin filaments that provide rigidity and plasticity for the plasma membrane, and the tight plasma membrane-cytoskeleton interface is the locus where receptors and signaling molecules (e.g. G-proteins, enzymes, etc.) are anchored, recruited or linked together to create and transmit biochemical signals. The oocyte surface is also covered with a myriad of microvilli filled with actin filaments that continually undergo treadmilling [46, 47]. The actin bundles in microvilli and the subplasmalemmal cortical layer drastically reorganize themselves during meiotic maturation of oocytes and upon fertilization, [47-51]. These cytoskeletal rearrangements in microvilli and subplasmalemmal layer are likely to affect the electrical and mechanical properties of the plasma membrane and the activities of the ion channels [52-54]. In parallel to the rearrangement of the actin cytoskeleton, ER exhibits microfilament-dependent movement during the meiotic maturation of oocytes [55]. The consequent repositioning of ER-studding ion channels during maturation might, in part, explain the oocytes' sensitization to $InsP_3$, which is inhibited by an actin drug, latrunculin-A (LAT-A) [27, 56, 57]. Examples of the ion channel and pump activities being modulated directly or indirectly by the neighboring actin cytoskeleton have been shown on various occasions [58-61], and we have also demonstrated that alteration of the cortical actin cytoskeleton by use of actin drugs, cofilin, or anti-depactin antibody causes significant changes to the intensities and patterns of the Ca^{2+} signals in the fertilized eggs of starfish and sea urchin [62-64]. Furthermore, the two distinct Ca^{2+} responses displayed by maturing oocytes of starfish at the time of meiotic reinitiation (a global wave, 1-2 min after hormone addition) and during germinal vesicle breakdown (Ca^{2+} influx spikes, 15-40 min after the stimulation) are also modulated by the polymerization status of the actin cytoskeleton [65, 66]. Hence, while intracellular Ca^{2+} signals change the actin cytoskeleton, actin filaments also modulate Ca^{2+} homeostasis in cells either by affecting ion channel activities or by directly serving as a high-affinity Ca^{2+} buffer and reservoir [67, 68].

In this discourse of reciprocal regulation between Ca^{2+} and the actin cytoskeleton, yet another distinct phenomenon has to be mentioned. LAT-A, which binds to actin monomer and thereby promotes depolymerization of actin filaments wherever F-actin turnover rate is high [69, 70], intriguingly induces fertilization-like Ca^{2+} waves and cortical flashes without the aid of sperm [46]. This seemingly 'spontaneous' and repetitive Ca^{2+} increase in response to LAT-A has been observed only in the mature eggs of *A. aranciacus* but not in the eggs of other species of starfish or sea urchin ever tested, and requires a time lag that matches the lead time for actin depolymerization [46].

In this communication, we have studied the molecular mechanism of LAT-A-induced egg activation. Our results indicated that it is PLCγ, and not $InsP_3$ receptor, whose activity was modulated by LAT-A following the structural alteration of the subplasmalemmal actin filaments. Hence, our study demonstrates the presence of another layer of control by which the actin cytoskeleton flexes its influence over the Ca^{2+} signaling machinery of the cell: modulation of the activity of the enzyme that synthesizes Ca^{2+}-mobilizing second messenger $InsP_3$.

Materials and Methods

Preparation of oocytes

Astropecten aranciacus were captured in the Gulf of Naples or at the sea near Gaeta during the breeding season (January to April) and transported to the *Stazione Zoologica* in Naples, Italy. Germinal vesicle (GV)-stage oocytes were obtained by a small slit on the central dorsal area of female adult animals, and transferred to filter-sterilized seawater. Individual oocytes released from the gonad were sieved in gauze and rinsed several times. To induce meiotic maturation, oocytes were stimulated with 10 μM 1-methyladenine (1-MA) in seawater for 70 min. The oocytes at this stage were referred to as 'eggs' in this study.

Actin drugs, chemicals, and reagents

LAT-A and Jasplakinolide were purchased from Molecular Probes, and phalloidin from Invitrogen. Cytochalasin B, U-73122, U-73343, neomycin, and all other chemicals and agents were purchased from Sigma-Aldrich, unless specified otherwise, e.g., mycalolide B (Santa Cruz Biotechnology). All chemicals and reagents were utilized as described in manufacturers' instruction.

Microinjection, photo-activation of caged $InsP_3$, and Ca^{2+} imaging

Oocytes were microinjected with various agents and dyes, as previously described [44, 47]. The pipette concentrations of fluorescent calcium dye (Calcium Green conjugated with 10 kDa dextran, Molecular Probes) and caged $InsP_3$ (Molecular Probe) prepared in the injection buffer (10 mM Hepes, 0.1M potassium aspartate, pH 7.0) were 5 mg/ml and 2 μM, respectively. The caged $InsP_3$ was photo-liberated by irradiating the eggs with 330 nm UV light by use of the computer-controlled shutter system Lambda 10-2 (Sutter Instruments, Co., Novato, CA). Cytosolic Ca^{2+} changes were recorded with a cooled CCD camera (MicroMax, Princeton Instruments, Inc., Trenton, NJ) mounted on a Zeiss Axiovert 200 microscope with a Plan-Neofluar 20x/0.50 objective. The quantified Ca^{2+} signal was normalized with the baseline fluorescence (F_0) following the formula $F_{rel} = [F\text{-}F_0]/F_0$, where F represents the average fluorescence level over the entire oocyte. The incremental changes of the Ca^{2+} rise was analyzed by applying the formula $F_{inst} = [(F_t\text{-}F_{t\text{-}1})/F_{t\text{-}1}]$ to visualize the site of instantaneous Ca^{2+} release. Fluorescent Ca^{2+} images were analyzed with MetaMorph software package 7.7 (Universal Imaging Corporation, West Chester, PA, USA).

Fluorescent fusion proteins ligated to the Pleckstrin Homology (PH) domain of rat PLC-δ1

The cDNA fragment encoding the PH domain (140 amino acid residues) that specifically interacts with PIP2 was prepared and fused to the expression vector (pET28, Novagen) containing GFP or RFP as described previously [47]. The fusion proteins expressed from the two plasmid were referred to as PH-GFP and RFP-PH, respectively, in respect of the configuration.

F-actin staining and confocal microscopy

F-actin was visualized in living oocytes by microinjecting AlexaFluor568-conjugated phalloidin (50 μM, pipette concentration) and examined with Zeiss LSM 510 META laser-scanning confocal microscope (Jena, Germany) by use of a Planar-Neofluar 25x/0.80 objective water lens through a BP 560/610 emission filter. On the other hand, PH-GFP was visualized by use of the same confocal microscope with excitation at 488 nm and emission at 500/555 nm, wheras LifeAct-GFP and RFP-SH2 were visualized by Leica TCS SP8 X with the WLL laser. Transmitted light and fluorescence confocal images were acquired from the equatorial planes.

Cloning of the Src Homology 2 (SH2) domains from A. aranciacus PLC-ɣ

The cDNA fragment encoding the tandem SH2 domains were cloned through RT-PCR by use of degenerate primers elected from the most conserved regions. To this end, the protein sequences of PLC-ɣ from diverse animal species were aligned (zebrafish, GenBank: AY163168; *Asterina miniata*, AY486068; sponge, BAA76275; human, ABB84466; *Paracentrotus lividus*, CAB38087; *Drosophila melanogaster*, BAA06189), and a pair of degenerate primers were prepared: the forward primer (5'- GCGCGGGAATTCGAyTGyTGGGAyGG -3') from the target amino acid residues DCWDG, and the reverse primer (5'-GCGCGCAAGCTTyTTnCCrTGrAACCA-3') from the peptide sequence WFHGK (note: n=A,G,C, or T; y=C or T; r= A or G). To facilitate subsequent PCR and cloning procedure, the primers respectively contained EcoRI or HindIII site (underlined), and six extra

nucleotides were added (G and C) at the 5' end. RNA extracted from *A. aranciacus* oocytes (TRI Reagent, Sigma) was converted to cDNA by use of Superscript reverse transcriptase (Invitrogen, Life Technologies), and PCR was performed with SuperMix High Fidelity (Invitrogen, Life Technologies). The amplicon was ligated to the pCRII-TOPO vector (Invitrogen, Life Technologies), and the clones were verified by DNA sequencing. The amplicon coded for 192 amino acid residues that were 93% identical to the corresponding region of *Asterina miniata* PLC-ɣ [38]. To extend to the cDNA region containing the two SH2 domain, another round of RT-PCR was performed with a gene-specific forward primer (5'-ATCATTCTGTCCATCGAGAACCAC-3') and the third degenerate reverse primer with a HindIII site (5'-GCGCGCAAGCTTrTCnCCyTTCCACCA-3'). Thus, the two rounds of RT-PCR identified a stretch of cDNA encoding 465 amino acids encompassing the two SH2 domains. Finally, the cDNA for two SH2 domain spanning 226 amino acid residues was obtained through a new RT-PCR by use of two gene-specific primers: forward 5'-CAGGATCCCCGAATGATGAGTTGCACTTCTCAGA-3' and reverse 5'-CAGGATCCTCACCCTCCCAGTCGGTCTACGATCTCTT-3.' After verification of DNA sequence, the cDNA for the two SH2 domains was cleaved by BamHI and ligated to the pET28 plasmid that contained RFP. The resulting plasmid and the expressed protein were referred to as RFP-SH2. On the other hand, the cDNA encoding only the monomeric RFP was ligated between the Bam HI and Hin dIII sites of pET28b (Novagen) [47]. The protein expressed from this plasmid was referred to as 'RFP' in this study. A sequential site-directed mutagenesis introduced to RFP-SH2 produced a missense mutant R586K/R694K [36], but the overexpressed protein had a strong tendency to go into the inclusion bodies or aggregate during dialysis. For this reason, RFP was used as the negative control for RFP-SH2. The purity and the ubiquitous subcellular distribution of the two proteins in the microinjected eggs were shown in Supplemental Data 1 (For all supplemental material see www.karger.com/doi/10.1159/000492523).

Bacterial expression and purification of the fusion proteins

E. coli strain BL21 was transformed with the plasmid and allowed to grow in the presence of kanamycin (50 µg/ml) and stimulated with IPTG (1 mM). The overexpressed fusion proteins were isolated and purified by use of the Nickel affinity chromatography (Chelating Sepharose Fast Flow, GE Health Care), as described previously [47]. The eluted proteins were dialyzed in molecular sieve tubes (Spectrum Labs) against the protein injection buffer (10 mM Hepes buffer, pH 7.4, 450 mM KCl) and concentrated in Amicon Ultra columns (Merck Millipore Ltd). Similarly, LifeAct-GFP was expressed from pET11-LifeAct-GFP (a generous gift from Dr. Alex McDougall, Sorbonne Universités, France) and purified in the same method, but using 50 µg/ml ampicillin.

PH-GFP microinjection and quantification of PIP2 labeling on the plasma membrane

Oocytes were stimulated with 10 µM 1-MA for 70 min and microinjected with 200 µM PH-GFP that was prepared as described previously [47]. To examine the changes of PIP2 labeling at the plasma membrane after LAT-A treatment, the fluorescent images were captured with the CCD camera at 1 min intervals after the addition of 6 µM LAT-A or the vehicle (0.1% DMSO) in the media. The level of fluorescence was quantified in a tight rectangular region of interest (16.24 µm x 1.27 µm) over the plasma membrane at the uppermost part of the randomly oriented egg images.

Enzyme-linked immunosorbent assay (ELISA)

After LAT-A treatment or fertilization, eggs were collected in Eppendorf tubes by brief microfuge (200 x *g* for 15 sec) to remove seawater. After aspirating supernatant, cell pellets were quickly frozen in liquid nitrogen and stored at -80°C. The cell pellets were homogenized in 200 µl PBS, and the soluble fraction was collected by centrifugation at 1,500 × *g* for 10 min. After BioRad protein assay, the amount of $InsP_3$ in the soluble fraction was quantified with the Inositol Trisphosphate ($InsP_3$) ELISA Kit in 96 well plates (MyBioSources, Cat. # MBS 006011), following the manufacturers' instruction and in reference to the calibration curve (linear, $R^2 = 0.9984$). The cellular concentration of $InsP_3$ was expressed in terms of pg $InsP_3$/mg protein.

Statistical analysis

The average and variation of the data were reported as 'mean ± standard deviation (SD)' in all cases in this manuscript. Oneway ANOVA and t-tests were performed by use of Prism 3.0 (GraphPad Software), and $P<0.05$ was considered as statistically significant. For ANOVA results showing $P<0.05$, statistical significance

of the difference between the comprising groups was assessed by *post hoc* tests.

Results

The intracellular Ca^{2+} increase induced by LAT-A has two distinct components: global Ca^{2+} waves and cortical flashes

As if fertilized, mature eggs of *A. aranciacus* exposed to 6 µM LAT-A manifested robust and bimodal intracellular Ca^{2+} increases in nearly all cases tested (Supplemental video 1 and 2). The planar speed of the LAT-A-induced Ca^{2+} wave (3.1 ± 1.3 µm/sec, n=29) was virtually the same as that in the fertilized eggs of the same batch: 2.6 ± 0.60 µm/sec (n=12), P=0.1311. As with fertilization, the Ca^{2+} wave evoked by LAT-A can originate from the subplasmalemmal zone in any part of the egg surface: 58.3 % in animal hemisphere, 41.7% in vegetal (n=24). Whenever detected, the cortical flashes were preceded by a small local increase of Ca^{2+} near the plasma membrane with the time interval of 8-20 sec. The cortical flash is dependent upon extracellular Ca^{2+}, as judged by its selective abolishment in calcium-free seawater [46]. We have now observed that verapamil (50 µM, 40 min), an inhibitor of voltage-gated Ca^{2+} channels, totally eliminates cortical flashes without significantly affecting the peak amplitude of the Ca^{2+} wave (1.02 ± 0.04 RFU for verapamil; 0.95 ± 0.05 RFU for the control; n=5 for each group, P=0.0584). Thus, the cortical flash after the LAT-A treatment is likely to be linked to the rapid changes of the membrane potential that are also known to take place in *A. aranciacus* eggs with the similar time lag in response to the same dose of LAT-A [71]. The LAT-A-induced global Ca^{2+} waves, on the other hand, were shown to be selectively suppressed by heparin, a conventional inhibitor of $InsP_3$ receptor [72-74] that did not affect the cortical flash [46]. However, later findings that the same dose

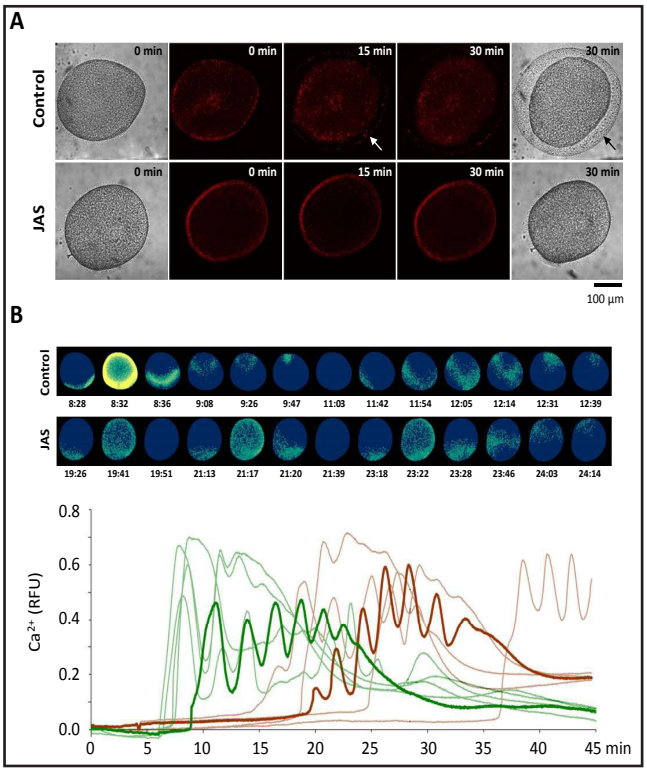

Fig. 1. LAT-A-induced activation of starfish eggs is inhibited by jasplakinolide. Mature eggs of *A. aranciacus* were microinjected with a low dose of AlexaFluor568-phalloidin (50 µM in pipette) to monitor the changes of the actin cytoskeleton in response to LAT-A (6 µM). (A) Prior to the exposure to LAT-A, the eggs were pretreated with either 12 µM jasplakinolide (JAS) or 0.05% DMSO (control) for 30 min. Actin filaments were visualized by confocal microscopy immediately before (t=0 min) and after (15 and 30 min) adding LAT-A to the media. The vitelline envelope was elevated by 15 min, as evidenced by the traces of actin bundles in the perivitelline space (white arrow). By 30 min, it was fully elevated as shown in the bright field view (black arrow). The structural changes of the egg actin cytoskeleton and the elevation of vitelline envelope were abolished by JAS pretreatment. (B) The pseudo-colored relative fluorescence images in the top panel represent the sites and extent of instantaneous Ca^{2+} increments in the eggs, which were calculated by applying the formula $F_{inst} = [(F_t - F_{t-1})/F_{t-1}]$ at the key time points (min:sec). The graph below depicts the trajectories of the intracellular Ca^{2+} level changes in the control (green curves) and the JAS-pretreated eggs (brown). The moment of LAT-A addition was set to t=0. To illustrate the repetitive nature of the Ca^{2+} waves, the trajectories of the two individual eggs featured in the upper panel were highlighted in bold lines.

Table 1. LAT-A-induced Ca^{2+} signals are significantly delayed by jasplakinolide and phalloidin. *Concentration in the microinjection pipette. Non-significant difference (n.s.)

	Administration	Time Lag	Ca^{2+} Peak	Cortical Flash	Wave Counts
0.05 % DMSO	media	14.58 ± 9.20 min (n=29)	0.69 ± 0.11 RFU	0.047 ± 0.049 RFU	3.72 ± 1.60
12 μM Jasplakinolide	media	21.20 ± 9.68 min (n=19)	0.62 ± 0.17 RFU	0.039 ± 0.031 RFU	3.26 ± 1.66
t- test		P<0.05	n.s.	n.s.	n.s.
DMSO	microinjection	11.25 ± 6.75 min (n=22)	0.74 ± 0.11 RFU	0.024 ± 0.043 RFU	3.0 ± 1.5
3 mM* Phalloidin	microinjection	19.42 ± 14.07 min (n=8)	0.69 ± 0.11 RFU	0.034 ± 0.033 RFU	2.3 ± 1.8
t-test		P<0.05	n.s.	n.s.	n.s.

of heparin inhibiting $InsP_3$ receptors also induces hyperpolymerization of cortical actin in starfish eggs [65, 75] complicated interpretation of the data regarding the source of the Ca^{2+} wave induced by LAT-A. That is, LAT-A-induced Ca^{2+} wave was inhibited either by repressing the activity of $InsP_3$ receptor or simply by stabilizing the cortical actin filaments.

The intracellular Ca^{2+} increase induced by LAT-A is inhibited or significantly delayed by agents stabilizing F-actin

To demonstrate that the LAT-A-induced Ca^{2+} waves and cortical flashes are due to the changes of the actin cytoskeleton, and not to some unknown side-effects of the drug, we tested whether the Ca^{2+} responses are prevented by the agents stabilizing F-actin. As shown in Fig 1A, starfish eggs exposed to 6 μM LAT-A underwent accelerated depolymerization of the cortical actin filaments. By 15 min, these eggs displayed signs of cortical granules exocytosis, i.e. elevation of the vitelline layer, which requires a massive increase of intracellular Ca^{2+}. When the eggs were pretreated with 12 μM jasplakinolide (JAS) prior to LAT-A exposure, the progressive depolymerization of subplasmalemmal F-actin was blocked, as judged by the AlexaFluor-phalloidin staining (Fig. 1A). Many of these eggs did not elevate vitelline layers. Indeed, the frequencies of the eggs exhibiting Ca^{2+} responses to LAT-A within 45 min dropped to 67.8 ± 1.92 % (based on three batches comprising 10 eggs in each group) from the values of the control eggs pretreated with 0.05% DMSO (96.7 ± 5.8%, N=3, P<0.01). Likewise, microinjection of phalloidin (PHAL) counteracted the net actin-depolymerizing effect of LAT-A by stabilizing the subplasmalemmal F-actin (Fig. 2A). Following microinjection of PHAL, the frequencies of the eggs displaying Ca^{2+} responses to

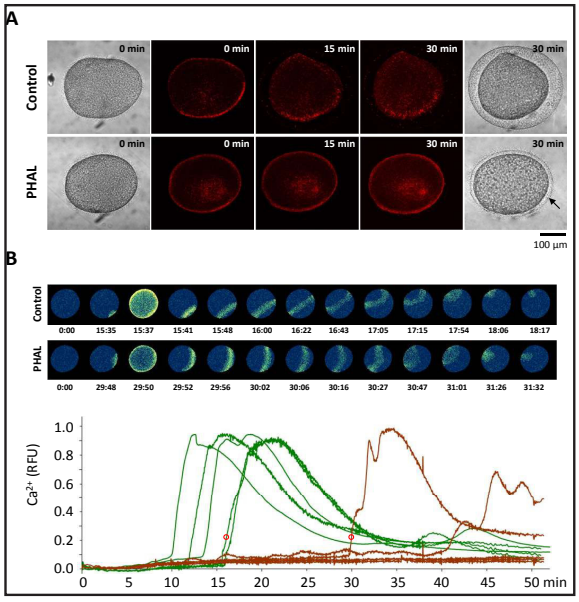

Fig. 2. LAT-A-induced intracellular Ca^{2+} increase is inhibited by phalloidin. (A) *A. aranciacus* oocytes were microinjected with calcium dyes to monitor the changes of the intracellular Ca^{2+} levels in response to LAT-A. Following meiotic maturation (10 μM 1-MA, 70 min), eggs were microinjected with 3 mM (concentration in the pipette) phalloidin (PHAL) or DMSO (control). After 20 min preincubation, the eggs were exposed to 6 μM LAT-A. Most eggs microinjected with PHAL failed to elevate the vitelline envelope, but few eggs displayed its partial elevation (arrow). (B) The pseudo-colored relative fluorescence images in the top panel represent the sites and extent of instantaneous Ca^{2+} increments in the eggs at the key time points (min:sec). The graph below depicts the trajectories of the Ca^{2+} level changes in the control (green curves) and the PHAL-microinjected eggs (brown). The moment of LAT-A addition was set to t=0. The Ca^{2+} trajectories of the individual eggs visualized in pseudocolor images in the upper panel were marked with small circles.

LAT-A was severely reduced to 35.6 ± 31.6% (based on 4 batches comprising 4-7 eggs) as opposed to the control eggs microinjected with DMSO (100 ± 0.0 %, N=4, P<0.01). Thus, PHAL overrode the actin-depolymerizing action of LAT-A (Fig. 2A) and precluded the Ca^{2+} response in the great majority of the cells. For those eggs treated with JAS or PHAL that still responded to LAT-A, the Ca^{2+} signal came out only after a significantly prolonged delay (Table 1). Once the Ca^{2+} response started, however, the major characteristic features of the Ca^{2+} waves and cortical flashes were not significantly altered by JAS or PHAL. Except for the increased time lag, neither the amplitudes of the Ca^{2+} waves and cortical flashes nor their multiplicity (wave counts) were significantly altered by the agents stabilizing F-actin (Table 1). Nonetheless, in some eggs microinjected with PHAL, the Ca^{2+} waves induced by LAT-A were atypical in a sense that the wave did not seemingly take a planar form but displayed a circular propagation pattern along the plasma membrane (Supplemental video 3). Hence, these results suggest that the LAT-A-induced Ca^{2+} increases are linked to the net depolymerization of cortical F-actin, but the inhibitory effect of the agents stabilizing F-actin was mainly to delay the Ca^{2+} responses rather than suppressing the individual elements of the Ca^{2+} increases.

LAT-A does not enhance sensitivity of $InsP_3$ receptors

In view of the fact that certain Ca^{2+} channels are embedded in the actin cytoskeleton, which modulates their activities of ion transmission [60, 76], one possible mechanism by which LAT-A induces intracellular Ca^{2+} rise is to change the micro-environment of the Ca^{2+} channels to the extent that the changes of their surrounding cytoskeletal elements eventually come to trigger a Ca^{2+} increase. For example, $InsP_3$ receptor is non-covalently linked to the actin filaments [77], and their positioning on the ER can be affected by changes of the actin cytoskeleton

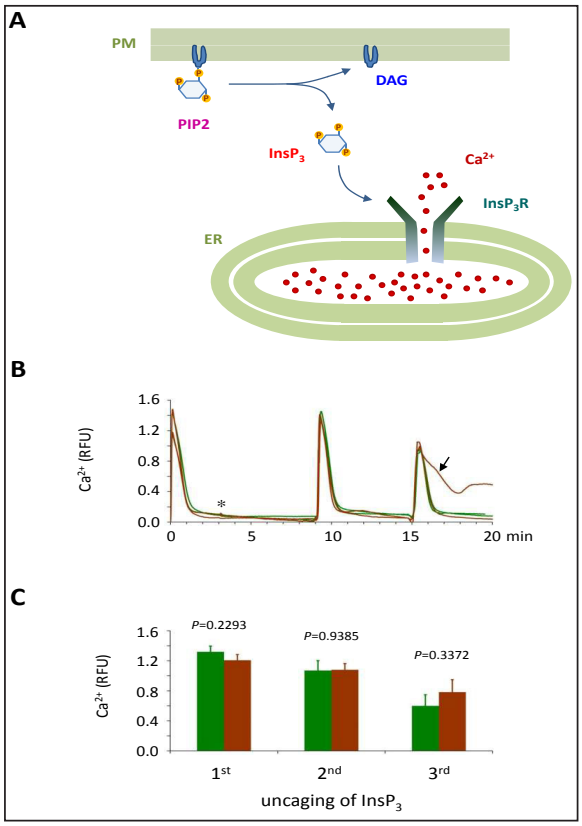

Fig. 3. LAT-A does not enhance sensitivity of $InsP_3$ receptors. (A) A schematic diagram of intracellular Ca^{2+} signaling through the PLC/$InsP_3$/$InsP_3$ receptor pathway. (B) Caged $InsP_3$ (2 μM, pipette concentration) was microinjected into *A. aranciacus* oocytes together with Calcium Green (50 μg/ml). After inducing meiotic maturation (10 μM 1-MA, 70 min), the caged $InsP_3$ was liberated inside the eggs by UV illumination (1st uncaging, 5 sec), and the Ca^{2+} response was monitored with a cooled CCD camera. Three minutes later, either 2 μM LAT-A or 0.01% DMSO (control) was added to the media, and the caged $InsP_3$ was sequentially liberated 6 and 12 minutes after the drug addition (2nd and 3rd uncaging: 10 and 27 sec, respectively). Brown curves depict the Ca^{2+} trajectories in the eggs treated with LAT-A, while green curves represent control eggs. Results from one of the three independent experiments were illustrated. The asterisk marks the moment of drug addition, and the arrow indicates contribution of an additional Ca^{2+} surge due to the effect of LAT-A, which was independent of the exogenous $InsP_3$. (C) Quantification of the Ca^{2+} responses during the 1st (trial), 2nd (6 min) and 3rd (12 min) uncaging. The average amplitude of the calcium peaks at each uncaging was calculated from six eggs treated in the same conditions. Green, the control eggs; Brown, the eggs treated with LAT-A. Error bars indicate standard deviation, and the P values above the paired bars indicate the results of the t-tests.

[78, 79]. Thus, it was conceivable that the LAT-A-induced cytoskeletal changes might have rendered the Ca^{2+} stores extremely sensitive to the background level of cytosolic $InsP_3$ and thereby catalyzed seemingly spontaneous release of Ca^{2+}. To explore this possibility, we tested if starfish eggs become progressively sensitive to exogenous $InsP_3$ during the course of the incubation with LAT-A. To this end, starfish eggs were preinjected with 2 μM of caged $InsP_3$, and the Ca^{2+}-mobilizing second messenger was photo-liberated at certain time intervals before the LAT-A-induced Ca^{2+} increase takes place (Fig. 3). With the same batch of eggs displaying nearly equal amount of Ca^{2+} releases upon $InsP_3$ uncaging before the drug addition, we found that LAT-A did not significantly increase the amplitude of the $InsP_3$-dependent Ca^{2+} releases until the eggs were about to manifest their own Ca^{2+} response to LAT-A (Fig. 3B, arrow). Hence, in the given experimental conditions, LAT-A did not appear to enhance the sensitivity of $InsP_3$ receptor itself.

Pharmacological inhibitors of phospholipase C abolish the LAT-A-induced Ca^{2+} increases

We then tested if LAT-A-induced Ca^{2+} increase is related to synthesis of $InsP_3$. This Ca^{2+}-mobilizing second messenger is produced by phospholipase C (PLC) that hydrolyzes phosphatidylinositol 4,5-bisphosphate (PIP2) to $InsP_3$ and diacylglycerol (Fig. 3A). As neomycin specifically binds to PIP2 [80, 81], it has been utilized as an inhibitor of PLC [82-84]. As shown in Fig 4A, microinjection of the eggs with neomycin (50 mM, pipette concentration) completely blocked the Ca^{2+} responses (both the cortical flash and global wave) to LAT-A in all cases tested (n=20), whereas the control eggs microinjected with the injection buffer exhibited the expected Ca^{2+} responses to LAT-A in 19 out of 20 eggs. Interestingly, the same dose of neomycin did not completely abolish the Ca^{2+} wave when the same batch of the microinjected eggs were fertilized (Fig. 4B), although the peak amplitude of the Ca^{2+}

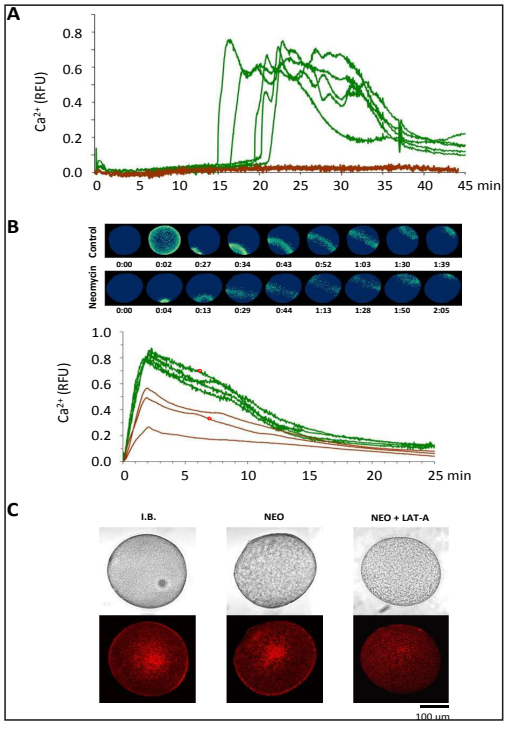

Fig. 4. LAT-A-induced Ca^{2+} increases are highly susceptible to neomycin. (A) *A. aranciacus* eggs loaded with calcium dyes were microinjected with either 50 mM neomycin (pipette concentration) or the injection buffer (control). After 20 min, the eggs were exposed to 6 μM LAT-A, and the changes of the cytosolic Ca^{2+} level were monitored from the moment of LAT-A addition (t=0). The Ca^{2+} trajectories in the control (green) and neomycin-injected eggs (brown curves, n=5) were presented from one of the three independent experiments showing similar results. (B) Ca^{2+} responses in the fertilized eggs that had been microinjected with 50 mM neomycin. Top: pseudo-colored relative fluorescence images of the instantaneous Ca^{2+} increments in the eggs at the key time points. Bottom: increases of the cytosolic Ca^{2+} levels in the control (green curves) and neomycin-injected eggs (brown curves) at fertilization. The time point immediately before the detection of the first Ca^{2+} response after fertilization was set to t=0. Results were obtained from the same batches of the eggs used for the LAT-A experiments, and one of the two independent experiments was presented. (C) Lack of the major structural changes of the actin cytoskeleton in the eggs microinjected with neomycin, as judged by live staining with AlexaFluor568-phalloidin. Mature eggs of *A. aranciacus* were microinjected with 50 mM neomycin (NEO) or the injection buffer (I.B.). Aliquots of neomycin-injected eggs were exposed to 6 μM LAT-A (NEO + LAT-A). After 30 min incubation, the eggs were microinjected for a second time with AlexaFluor568-phalloidin (50 μM in pipette) to visualize F-actin in confocal microscopy.

wave was significantly reduced (0.54 ± 0.05 RFU, n=8) in comparison with the control (0.77 ± 0.094 RFU, n=11, P<0.001). Since total abolishment of the fertilization Ca^{2+} waves in this batch of eggs required a higher dose of neomycin (e.g. 500 mM), it appears that the LAT-A-induced Ca^{2+} increases are much more susceptible to the PLC inhibitor in comparison with the Ca^{2+} wave produced in fertilized eggs. Curiously, neomycin had also a tendency to suppress the short lived cortical flash in the fertilized starfish eggs (Fig. 4B). Whether this reflects non-specificity of the drug or not, it is important to note that neomycin completely suppressed the LAT-A-induced Ca^{2+} waves and cortical flashes without displaying interference with the subplasmalemmal actin dynamics (Fig. 4C) unlike the cases with JAS and PHAL (Fig. 1 and 2). In other words, F-actin was still depolymerized by LAT-A, but no Ca^{2+} waves nor egg activation were observed in the eggs pretreated with neomycin, suggesting that F-actin disassembly *per se* may not be the direct cause of the Ca^{2+} increase. The same results were corroborated by use of another PLC inhibitor U-73122. As shown in Fig. 5A, preincubation of the eggs with 10 μM U-73122 prior to LAT-A exposure completely blocked the Ca^{2+} response that was observed in the control eggs pretreated with a structurally related but non-functional drug U-73343. Again, under the given experimental condition, U-73122 did not appreciably change the structure of the subplasmalemmal actin cytoskeleton, nor interfere with its depolymerization by LAT-A (Fig. 5B). However, interpretation of these data may call for cautions as to the specificity of the drugs. Neomycin inhibits not only PLC but also phospholipase D (PLD) that targets phosphatidylcholine [85], and U-73122 has been questioned as to its precise mode of action. Besides its inhibitory effects on PLC, U-73122 reportedly acts on several ion channels and pumps transmitting Ca^{2+} presumably by alkylating the proteins [86-90], and may interfere with fine regulation of cellular F-actin or actin-binding proteins [65, 91, 92]. In this regard, the idea that the LAT-A-induced Ca^{2+} rise was mediated by increased production of $InsP_3$ was put to further tests by use of microinjection of recombinant proteins specifically targeting PLC or PIP2.

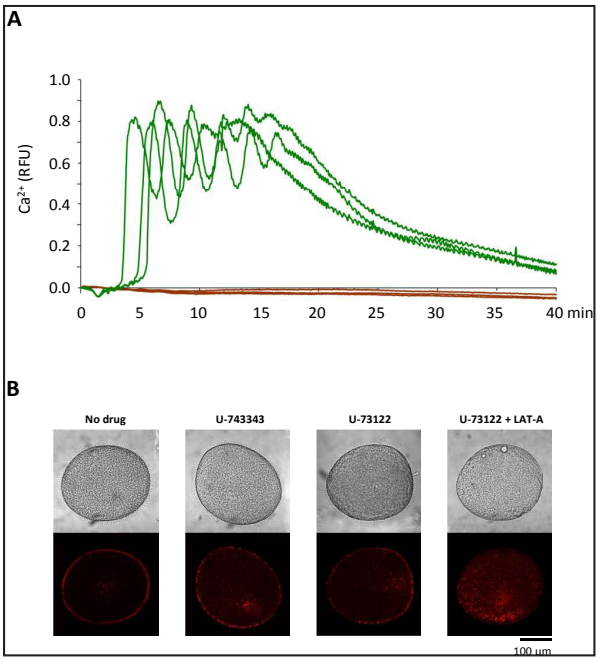

Fig. 5. LAT-A-induced Ca^{2+} increase is abolished by U-73122. (A) *A. aranciacus* eggs preinjected with calcium dyes were incubated for 30 min in the presence of 10 μM U-73122 or its closely related analogue that does not inhibit phospholipase C (U-73343, 10 μM). The eggs were then exposed to 6 μM LAT-A, and the changes of the cytosolic Ca^{2+} level were monitored. The Ca^{2+} responses in the eggs pretreated with U-73122 and U-73343 (control) were shown in brown and green trajectories, respectively. Representative results of three independent experiments were illustrated. (B) Lack of the major structural changes of the actin cytoskeleton in the eggs incubated with U-73122 or U-73343. *A. aranciacus* eggs were microinjected with a low dose of AlexaFluor568-phalloidin (50 μM, pipette concentration) and exposed to either 10 μM U-73122 or U-73343 (control). Actin filaments were visualized by confocal microscopy immediately before (0 min) and 30 min after the addition of the drugs.

Dominant negative mutant protein constructed from A. aranciacus PLC-ɣ selectively suppresses the LAT-A-induced Ca^{2+} waves, but not the cortical flashes

Ca^{2+} waves in fertilized egg of starfish heavily depend on PLC-ɣ [38]. To inhibit the endogenous activity of PLC-ɣ, the cDNA fragment containing the two SH2 domains of PLC-ɣ (Fig. 6A) was cloned from *A. aranciacus* oocytes and fused to RFP as described in Materials and Methods. When the bacterially expressed protein (RFP-SH2) was microinjected into the eggs, subsequent fertilization failed to display propagation of the Ca^{2+} wave, although spermatozoa interacting with the egg in the media fired a cortical flash and initiated multiple abortive Ca^{2+} spots near the egg surface (Fig. 6B arrows). Thus, RFP-SH2 did not suppress the generation of the initial Ca^{2+} increase but selectively inhibited the *spread* of the Ca^{2+} wave. When the eggs microinjected with the same amount of RFP-SH2 (375 µM concentration in pipette) were exposed to 6 µM LAT-A, comparable effects were observed. As shown in Fig. 6C, the global Ca^{2+} wave was selectively suppressed while cortical flashes were saved in these eggs. The peak amplitude of the Ca^{2+} waves in the eggs microinjected with RFP-SH2 averaged 0.25 ± 0.18 RFU (n=16), whereas that of the control eggs (microinjected with RFP) was 1.13 ± 0.19 RFU (n=16, P<0.0001). In contrast, occurrence of the cortical flashes was not affected by RFP-SH2, as 10 out of 16 eggs manifested cortical flashes even when no sign of global Ca^{2+} waves was detected (Fig. 6C). The average amplitude of the cortical flashes in these eggs (0.10 ± 0.10 RFU) was somewhat lower than that of the control eggs (0.18 ± 0.069 RFU, n=5), but the difference was not statistically significant (P=0.1210).

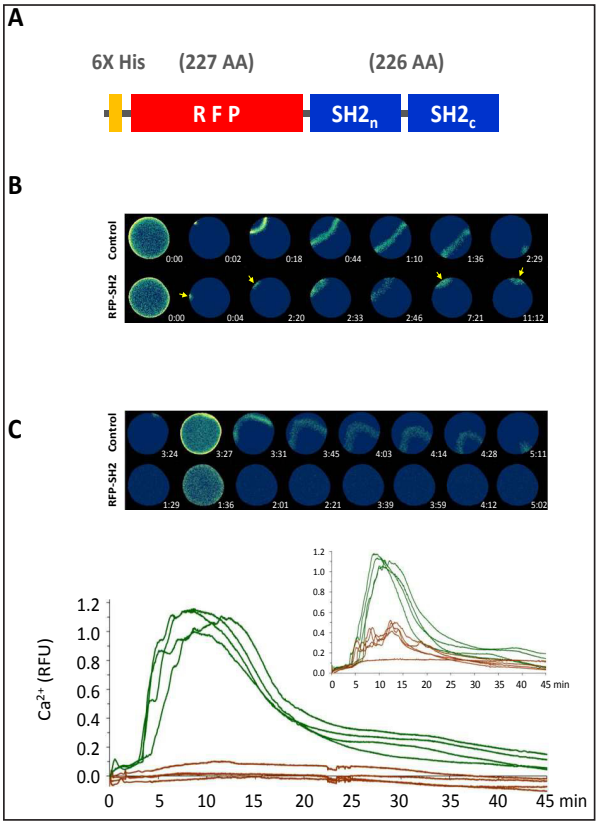

Fig. 6. Dominant negative mutant protein containing the two SH2 domains of PLC-ɣ inhibits the LAT-A-induced Ca^{2+} waves, but not the cortical flashes. (A) The tandem SH2 domains were cloned from the PLC-ɣ mRNA of *A. aranciacus*, and the cDNA was fused to bacterial expression vector of RFP as described in Materials and Methods. Starfish eggs charged with calcium dyes were then microinjected with either 375 µM RFP-SH2 fusion protein or the same molarity of RFP (control), and its effect on intracellular Ca^{2+} signaling was tested 20 min later by fertilization or exposure to 6 µM LAT-A. (B) The pseudo-color images representing the instantaneous Ca^{2+} increments in the fertilized eggs. In the control eggs, a single Ca^{2+} wave originated from one spot and continuously propagated to the antipode. In contrast, the Ca^{2+} signals failed to form a wave in the eggs microinjected with RFP-SH2 despite the multiple trials at the egg-sperm interaction sites (arrows). The moment of the first detectable Ca^{2+} response was set to t=0 (about 10 sec after sperm addition). (C) Eggs exposed to 6 µM LAT-A after the microinjection of RFP-SH2. In the majority of cases, RFP-SH2 completely abolished the LAT-A-induced Ca^{2+} wave (save cortical flashes) that was observed in the control eggs. The bigger graph below the pseudo-color images of the instantaneous Ca^{2+} increments depict the trajectories of the changes of the Ca^{2+} levels in the majority of eggs microinjected with RFP-SH2 (brown curves) or control proteins (green). In the inset were represented the Ca^{2+} responses in an independent batch of eggs. The moment of LAT-A addition was set to t=0.

Dose-dependent effects of RFP-PH on LAT-A-induced Ca^{2+} increases

The Pleckstrin Homology (PH) domain of mammalian PLC-δ1 has been used as a specific molecular tool to label or sequester PIP2, which is the substrate of PLC [93-96]. Furthermore, the PH domain of PLC-δ1 binds to $InsP_3$ with even higher affinity (K_d = 2 x 10^{-7} M) compared with PIP2 (K_d = 1.7 x 10^{-6} M) [97]. Thus, RFP-PH at higher doses is expected not only to inhibit PLC but also to buffer cytosolic $InsP_3$. As another way to test if LAT-A-induced Ca^{2+} increases involve the PLC-$InsP_3$ signaling pathway, we microinjected the eggs with RFP-PH fusion protein or its control protein that does not bind to PIP2 (R40A mutant). When microinjected at a low dose (200 μM, concentration in the pipette), RFP-PH did not suppress the LAT-A-induced Ca^{2+} wave nor cortical flash, but significantly delayed the onset of the Ca^{2+} response after the administration of LAT-A: 30.1 ± 11.4 min for the eggs with RFP-PH, and 10.5 ± 6.6 min for the control eggs; n=8 each, P<0.001 (Fig. 7A). On the other hand, when eggs were microinjected with a high dose (400 μM) of RFP-PH prior to LAT-A exposure, both Ca^{2+} waves and cortical flashes were abolished to the background noise levels (Fig. 7B).

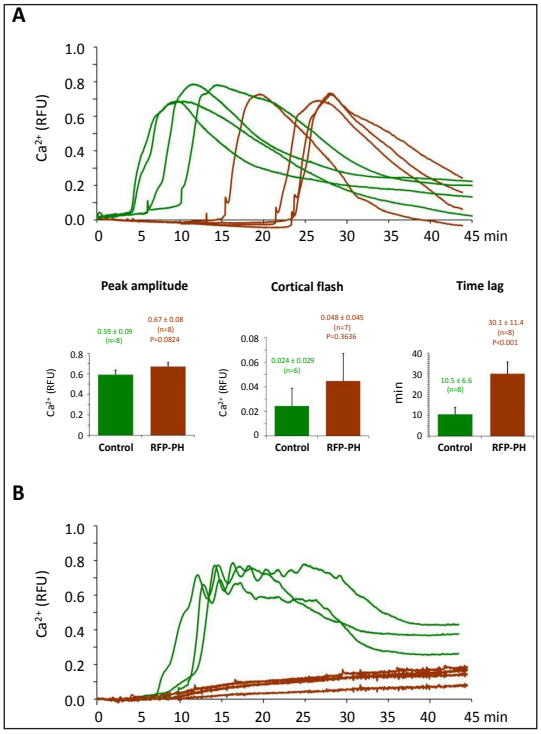

Fig. 7. Effects of the RFP-PH fusion protein on the LAT-A-induced Ca^{2+} increase in starfish eggs. (A) Low dose effects. *A. aranciacus* eggs loaded with calcium dyes were microinjected with either 200 μM RFP-PH fusion protein or its R40A mutant protein that does not bind to PIP2 (control). After 20 min incubation, the eggs were exposed to 6 μM LAT-A to monitor cytosolic Ca^{2+} changes. The Ca^{2+} trajectories in the eggs microinjected with RFP-PH (brown curves) and in the control eggs (green curves) were presented from one of the two independent experiments showing similar results. Histograms: the average of the Ca^{2+} peak amplitude (left), cortical flash (middle), and the time lag before the onset of the first Ca^{2+} wave (right) in response to LAT-A. (B) High dose effects. The eggs were microinjected with 400 μM RFP-PH or its control protein R40A. Whereas the control eggs microinjected with the high dose of R40A displayed normal Ca^{2+} trajectories (green curves), the eggs microinjected with the same amount of RFP-PH fail to produce a Ca^{2+} wave in response to LAT-A (brown curves). The Ca^{2+} trajectories were presented from one of the two independent experiments showing similar results.

LAT-A induces translocation of PH-GFP from the plasma membrane

The experimental data above obtained with inhibitors of PLC suggest that the LAT-A-induced Ca^{2+} waves in starfish eggs may be mediated by activation of PLC. If this is true, it is expected that incubation of the eggs with LAT-A somehow stimulates hydrolysis of PIP2, which is mostly located in the inner leaflet of plasma membrane lipid bilayer (Fig. 3A). We tested this idea by microinjecting eggs with a low dose of PH-GFP (150 μM pipette concentration), which specifically binds to PIP2 and $InsP_3$ with high affinity. At high concentration, this fusion protein inhibits access of PLC to PIP2 [95]. However, a low dose of the same protein has been used as a fluorescent probe to demonstrate a decrease of PIP2 on the plasma membrane [47, 98, 99]. If LAT-A induces hydrolysis of PIP2, such changes should be detected as a reduction of PH-GFP labeling on the plasma membrane. When microinjected into starfish eggs, PH-GFP predominantly labeled PIP2 on the plasma membrane (Fig. 8B). As expected, its fluorescence on the plasma membrane progressively declined after the

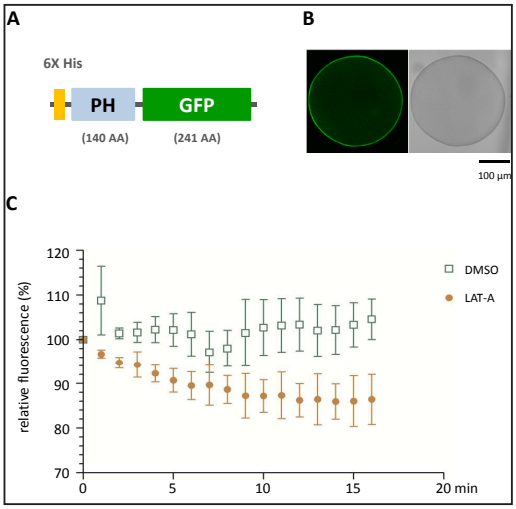

Fig. 8. LAT-A induces translocation of PH-GFP from the plasma membrane of starfish eggs. *A. aranciacus* eggs were microinjected with PH-GFP (150 µM, pipette concentration) that specifically binds to PIP2 on the inner leaf of the plasma membrane. (A) Configuration of the fluorescent probe for PIP2. (B) A confocal microscopic image and the bright field view of the egg showing the specific localization of PH-GFP on the plasma membrane. (C) Changes of the fluorescence level on the plasma membrane following the exposure of the eggs to 6 µM LAT-A or 0.1% DMSO (control). Fluorescence at the plasma membrane was quantified at 1 min intervals as described in Materials and Methods, and was normalized with the value in the same egg at the time of drug addition (t=0). Relative scores at each time point were averaged from 4 eggs for each treatment: filled circles (eggs exposed to LAT-A) and squares (control eggs treated with DMSO). Error bars indicate standard deviation (n=4).

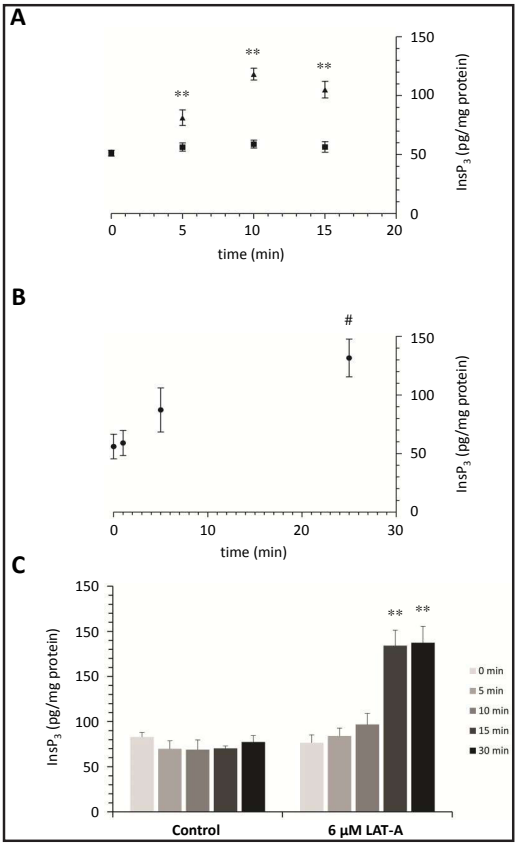

Fig. 9. Quantification of intracellular $InsP_3$ by ELISA. (A) Eight batches of *A. aranciacus* eggs were incubated with 6 µM LAT-A (closed triangles) or 0.1% DMSO (control, closed squares), and aliquots were collected for analysis at 5 min intervals, as described in Materials and Methods. Eggs immediately before drug addition was set as t=0. Post-hoc analysis: **P<0.01 in comparison with the values at t=0. (B) Control experiments with three batches of fertilized eggs (*A. aranciacus*). After adding sperm, aliquots of zygotes were collected at certain time points. Eggs immediately before sperm addition was set as t=0. Closed circles with error bars represent the mean ± SD of the $InsP_3$ concentration at each time point. Post-hoc analysis: #P<0.05 in comparison with the values at t=0 (C) Parallel experiments with sea urchin (*Paracentrotus lividus*) eggs incubated with 6 µM LAT-A or 0.1% DMSO (control). Post-hoc analysis: **P<0.01 in comparison with the values at t=0.

addition of LAT-A in the media. This is not due to time-dependent bleaching of the fluorescent probe because the PIP2 labeling on the plasma membrane did not change in the control eggs exposed to the vehicle of the actin drug (0.1% DMSO) (Fig. 8C). The evident decrease of PIP2 in the plasma membrane of the eggs incubated with LAT-A by the time of intracellular Ca^{2+} increase, i.e. 5-10 min, supports the idea that LAT-A somehow promotes PIP2 hydrolysis.

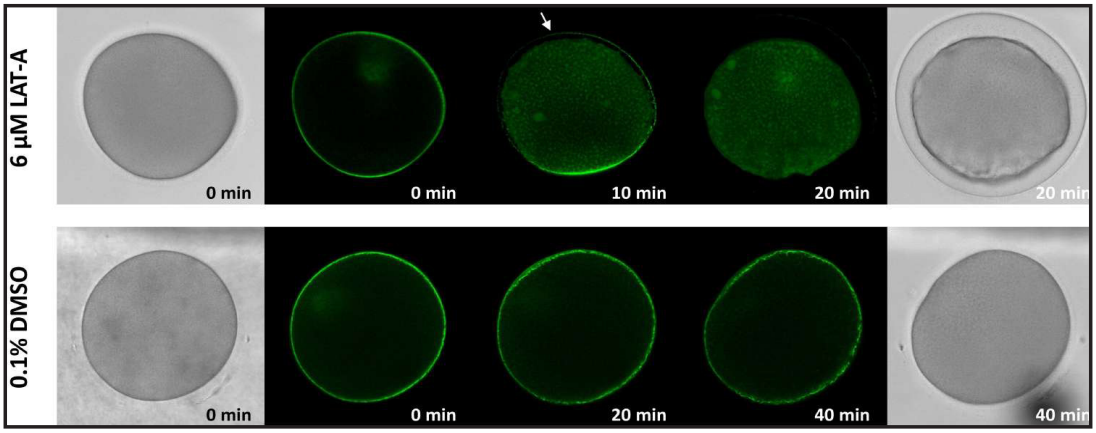

Fig. 10. Massive depolymerization of subplasmalemmal actin filaments in the starfish eggs exposed to LAT-A. *A. aranciacus* eggs microinjected with LifeAct–GFP fusion protein (6 µg/µl, pipette concentration) were exposed to 6 µM LAT-A or to the solvent of the drug (0.1% DMSO, final concentration), and the changes of the actin filaments were monitored by confocal microscopy. Whereas LAT-A induced extensive depolymerization of subplasmalemmal actin filaments by 10 min (arrow), the control eggs exposed to 0.1% DMSO lacked such changes even after extended incubation. Thus, the drastic changes of the actin filaments and egg activation are due to the legitimate effect of the actin drug, and not to the spontaneous changes of the actin cytoskeleton or to the side effect of DMSO.

LAT-A increases intracellular level of $InsP_3$

To corroborate the notion that LAT-A stimulates hydrolysis of PIP2, we have tested if incubation of the starfish eggs with the same dose of LAT-A actually leads to the increase of $InsP_3$ during the same time course. To this end, starfish eggs were exposed to 6 µM LAT-A, and the changes of intracellular levels of $InsP_3$ were monitored by ELISA. As shown in Fig. 9A, the $InsP_3$ level in the control eggs incubated with 0.1% DMSO remained the same throughout the 15 min incubation period ($P<0.4835$). In contrast, the eggs exposed to LAT-A exhibited a clear sign of time-dependent changes of intracellular $InsP_3$ contents after the drug addition ($P<0.0001$), as the $InsP_3$ level significantly arose by 5 min of incubation and reached its peak at 10 min. Thus, $InsP_3$ sharply increased during the time when the LAT-A-exposed eggs displayed intracellular Ca^{2+} increase with the concomitant decrease of plasma membrane PIP2, i.e. 5-10 min after the drug addition, which also coincides with massive depolymerization of subplasmalemmal actin filaments (Fig. 10). The peak concentration of $InsP_3$ observed in the eggs exposed LAT-A was similar to that in the fertilized eggs which were included in the assay as a control (Fig. 9B). Interestingly, the increase of cytosolic $InsP_3$ contents in response to LAT-A was not restricted to *A. aranciacus* eggs. While 6 µM LAT-A did not activate sea urchin eggs (*P. lividus*), as judged by the lack of a Ca^{2+} increase or elevation of the vitelline envelope, the same treatment surprisingly induced a sharp twofold increase of $InsP_3$ during the interval from 10 to 15 min (Fig. 9C). One explanation to this intriguing discrepancy is that eggs of different echinoderm species may have substantially variable sensitivity to $InsP_3$. According to the microinjection titration assay, sea urchin eggs (*P. lividus*) were far less sensitive than the eggs of starfish (*A. aranciacus*) to the microinjected $InsP_3$, at least by one order of magnitude (Table 2). Taken together, these results suggest that the induction of $InsP_3$ in echinoderm eggs by depolymerization of cortical actin might rather be more universal, but its effect on the internal Ca^{2+} stores may be masked by other factors.

Table 2. Comparison of starfish and sea urchin eggs for their sensitivity to $InsP_3$

		$InsP_3$ (pipette concentration)		
Eggs	Elevation of vitelline layer	1 μM	10 μM	100 μM
Starfish (*A. aranciacus*)	Full elevation	0 %	100 %	100 %
	Partial elevation	3 %	0 %	0 %
	No elevation	97 %	0 %	0 %
		(n=33)	(n=9)	(n=15)
Sea urchin (*P. lividus*)	Full elevation	0 %	0 %	74 %
	Partial elevation	0 %	0 %	21 %
	No elevation	100 %	100 %	5 %
		(n=22)	(n=10)	(n=19)

Discussion

Ca^{2+} is one of the most versatile second messengers inside cells whose instructive biochemical messages are decoded into a variety of cell functions such as muscle contraction, enzyme activation, gene regulation, secretion, neurotransmission, gametes activation, and so on [100]. While the intracellular Ca^{2+} increase is often visualized as waves or oscillations, a growing body of evidence suggests that the actin cytoskeleton may modulate the spatiotemporal trajectory of the Ca^{2+} signals in diverse cells, as exemplified by IgG-dependent Ca^{2+} increases in neutrophil and Jurkat T cells [101, 102], Ca^{2+} transients induced by bradykinin or mechanical force in aortic epithelial cells [103, 104], FcεRI-mediated Ca^{2+} increases in RBL-2H3 mast cells [105], the membrane depolarization-induced Ca^{2+} rise in neurons [106-108], maturation hormone-induced Ca^{2+} signals in oocytes [65, 66, 109], and sperm-induced Ca^{2+} increases in fertilized eggs [62-64, 75]. Whereas the actin cytoskeleton in most of these cases was shown to enhance or repress the Ca^{2+} signals that are normally induced by physiological stimuli, the Ca^{2+} signals featured in this communication regard a bimodal Ca^{2+} response evoked by LAT-A alone. This seemingly spontaneous phenomenon is not likely to be a side-effect of LAT-A, a relatively new actin drug [69], because two other drugs promoting actin depolymerization by different mechanisms, i.e. cytochalasin B and mycalolide B, produced comparable Ca^{2+} responses albeit with slightly lower efficiency (Table 3). Similarly, RBL-2H3 mast cells sensitized by IgE readily manifest Ca^{2+} oscillations in response to cytochalasin D or Mycalolide B within few minutes [110], suggesting that the intracellular Ca^{2+} increase linked to actin disassembly may not be restricted to certain species of starfish eggs.

In the present communication, we have studied the molecular mechanism that enables LAT-A to evoke intracellular Ca^{2+} increase in starfish eggs (*A. aranciacus*). As aforementioned, the Ca^{2+} signals induced by LAT-A have two components: Ca^{2+} influx (cortical flash) and the release from internal stores (global wave). The cortical flash was shown to be dependent upon external Ca^{2+} [46], and linked to the Ca^{2+}-dependent action potentials breaking out 5-10 min after the administration of LAT-A [71]. While the abolishment of the cortical flash by verapamil (see the text in Results) indicates L-type Ca^{2+} channels as its source, the mechanism by which the main global wave is generated by LAT-A was rather obscure and therefore became the main focus of our study. Because the LAT-A-induced Ca^{2+} increases were inhibited by actin drugs stabilizing actin filaments, i.e. JAS and PHAL (Fig. 1 and 2) and were mimicked by other actin drugs destabilizing actin filaments, i.e. cytochalasin B and mycalolide B (Table 3), it was clear that the Ca^{2+} signals evoked by LAT-A were the consequence of disassembly of cortical actin filaments. However, the inhibition of the LAT-A-induced Ca^{2+} signals by stabilizing cortical actin filaments was not absolute, as 67% of the JAS-treated eggs and 35% of the PHAL-microinjected eggs still exhibited the expected Ca^{2+} responses, albeit much more belatedly. In these eggs, neither the wave counts nor the amplitudes of the Ca^{2+} peaks and cortical flash were affected by the drugs stabilizing actin filaments (Table 1). Hence, it could be said that the main effect of JAS and PHAL on the LAT-A-induced Ca^{2+} signals is to cause significantly long or indefinite delay to the response, but not to suppress the Ca^{2+} trajectory itself. This observation raised a possibility that something else might be

Table 3. Induction of the Ca^{2+} increases by other drugs promoting depolymerization of actin filaments. *Refers to the maximal background noise. n/a = non-applicable

Actin Drugs	Time Lag	Eggs with Ca^{2+} response	Ca^{2+} Peak	Wave Counts
Cytochalasin B				
0 μM (0.1% DMSO)	n/a	0 % (n=8)	0.053 ± 0.033 RFU*	0
10 μM	4.45 ± 3.25 min	81.8% (n=11)	0.60 ± 0.13 RFU (n=9)	3.56 ± 1.67 (in 30 min, n=9)
Mycalolide B				
0 μM (0.6% DMSO)	n/a	0 % (n=9)	0.099 ± 0.052 RFU* (n=9)	0
6 μM	13.2 ± 4.03 min	60 % (n=10)	0.49 ± 0.29 RFU (n=6)	2.16 ± 1.16 (in 30 min, n=6)

under the surface to account for the generation of the Ca^{2+} signals, and that the unknown mechanism is modulated by disassembly of actin filaments. Previous work demonstrating total elimination of the LAT-A-induced Ca^{2+} waves by heparin suggested that $InsP_3$ receptor might be its source [46]. As $InsP_3$ receptors are known to become more sensitive to its ligand during oocyte maturation in an actin-dependent manner [56, 57], it was conceivable that LAT-A somehow rendered the eggs hypersensitive to $InsP_3$ while cortical actin filaments were disassembled. We tested this idea first, but found no evidence that the amount of the Ca^{2+} released by the same dose of uncaged $InsP_3$ becomes appreciably higher in the LAT-A treated eggs than in control eggs during the course of progressive disassembly of cortical actin filaments (Fig. 3). We then examined the upper end of the PLC/$InsP_3$/$InsP_3$ receptor signaling pathway (Fig. 3A), and found that the two pharmacological agents inhibiting the enzyme activity of PLC, i.e. neomycin and U-73122, totally eliminated the LAT-A-induced Ca^{2+} increases (Fig 4 and 5): an effect much stronger than the inhibition by JAS and PHAL that blocked actin dynamics (Fig. 1 and 2). In line with that, microinjection of a recombinant protein, which was constructed from the tandem SH2 domains of *A. aranciacus* PLCγ as a dominant negative mutant of the endogenous PLCγ (i.e. RFP-SH2), selectively abolished the global Ca^{2+} waves without affecting cortical flashes (Fig. 6). Unlike the eggs that escaped the inhibitory effects of JAS and PHAL (Fig. 1 and 2), a batch of eggs showing partial inhibition by RFP-SH2 exhibited Ca^{2+} waves with much reduced amplitude instead of prolonged time lag (Fig. 6C, inset). These results strongly suggested that disassembly of cortical actin filaments may evoke Ca^{2+} increase by enhancing the activity of PLC to produce $InsP_3$. This notion was further tested by microinjection of a fusion protein containing the PH domain of PLC-δ1 (i.e. RFP-PH) that specifically binds to PIP2 and thereby hampers the access of PLC to its substrate. As expected, low dose of RFP-PH (200 μM) delayed the LAT-A-induced Ca^{2+} increases, while a higher dose (400 μM) completely abolished them (Fig. 7). To test if LAT-A really promotes hydrolysis of PIP2, eggs were microinjected with a lower dose (150 μM) of the same PH domain fused to GFP in different orientation (i.e. PH-GFP), which was used as a fluorescent marker for PIP2. As expected, the labeling of PIP2 on the plasma membrane was progressively reduced during the course of LAT-A incubation (Fig. 8). This result is in line with the idea that plasma membrane PIP2 was gradually hydrolyzed to $InsP_3$ while cortical actin filaments were disassembled. Indeed, the direct biochemical assay by use of ELISA indicated that the cell content of $InsP_3$ was significantly increased 5-10 min after the incubation with LAT-A (Fig. 9). Interestingly, however, sea urchin (*P. lividus*) eggs, which do not display Ca^{2+} increases nor egg activation in response to LAT-A, exhibited comparable increases of cellular $InsP_3$ concentration (Fig. 9C). Thus, induction of $InsP_3$ by actin filaments disassembly might not be unusual for echinoderm eggs. On the other hand, the fact that *P. lividus* egg is much less sensitive to $InsP_3$ (Table 2), explaining the lack of Ca^{2+} response to LAT-A in these eggs, renders a support to the idea that Ca^{2+}-mobilizing second messengers might be buffered by other factors that modulate their function [111-113].

Although the experiments with neomycin, U-73122, RFP-SH2, and RFP-PH (Fig. 4-7) all indicate that PLC is instrumental in generating Ca^{2+} signals in response to LAT-A, it cannot be ruled out that LAT-A might have increased $InsP_3$ by attenuating the activity of inositol 1,4,5-trisphosphate 3-kinase (IP3K) [114]. However, increasing $InsP_3$ in this pathway alone would not have changed the PIP2 levels in the plasma membrane (Fig. 8). It is also possible

that the Ca^{2+} increase induced by disassembly of actin filaments may involve other second messengers such as cADPr [115], but the total elimination of the signals by the agents inhibiting PLC argues against that (Fig. 4 to 7). Alternatively, Ca^{2+} might have derived directly from the actin filaments themselves during disassembly. In this model, due to the high affinity to G-actin (K_d = 2x10^{-9} M), excess Ca^{2+} may be incorporated into polymerizing actin filaments and stored. It can be later released into cytosol when and where the actin filaments are depolymerized [67, 116]. It is conceivable that the Ca^{2+} ions released during oocyte maturation may be incorporated into newly formed actin filaments and then be liberated as the actin filaments are disassembled in response to LAT-A. However, this model is not compatible with the fact that LAT-A does not induce Ca^{2+} increases in the eggs of *Asterina pectinifera*, the species whose oocytes manifest much stronger Ca^{2+} responses during maturation than those of *A. aranciacus* [65, 66], although it cannot be ruled out that eggs of *A. pectinifera* did not display the Ca^{2+} signals because eggs of different animal species may have different actin dynamics. Taken together, all these data and considerations are compatible with a model in which LAT-A-induced disassembly of actin filaments increases synthesis of Ca^{2+}-mobilizing second messenger $InsP_3$ by stimulating PLC.

Induction of $InsP_3$ and Ca^{2+} signals by disassembly of actin filaments is not restricted to the starfish eggs of certain species. Earlier studies indicated that treatment of murine B lymphocytes with cytochalasin led to an increase of $InsP_3$ and the consequent intracellular Ca^{2+} release [117, 118]. As with eggs, it is noteworthy that the surface of lymphocytes is covered with actin-filled microvilli [119, 120]. While it is not clear how disassembly of cortical actin filaments can activate PLC, there have been intermittent reports suggesting that PLC is physically associated with cytoskeleton in various cells such as platelets [121, 122], fibroblasts [123], hepatocytes [124], macrophage precursors [125], as well as in plant cells [126]. In addition, Src-family kinases are also bound to the cytoskeleton as was shown in nerve growth cones, which are enriched with actin [127]. If both PLC and Src-family kinase are associated with the actin cytoskeleton and the generation of a Ca^{2+} wave requires interactions between the two, as was seen in fertilized eggs of starfish [39], physical changes of the actin cytoskeleton may serve a way to modulate the activity of PLC by putting the two enzymes in contact or keeping them distant from each other. Indeed, the tandem SH2 domains of PLCγ directly bind to actin *in vitro* [122, 125, 128] and to the actin cytoskeleton [123]. The SH2 domains not only bind to actin [125, 128] but also anchor PLCγ to a tyrosine kinase that in turn phosphorylates a specific tyrosine residue of PLCγ in the hinge domain [129]. Drastic changes to suboolemmal actin filaments, as was seen in the eggs fertilized or exposed to LAT-A, would put an end to the quiescent control that keeps the signaling molecules dormant. Disassembled actin filaments are also expected to give way for PLC to access its substrate PIP2 more freely in the plasma membrane, and the liberated G-actin may help to dislodge profilin that would otherwise mask PIP2 [130, 131]. In future studies, it would be of interest to test this model postulating suboolemmal actin filaments as a 'scaffold' that modulates the enzyme activity of PLC following the transmitted external stimuli.

Like a fertilizing sperm, LAT-A can induce both cortical flash and global Ca^{2+} wave in starfish eggs, but there are several important differences. Whereas the fertilized eggs display the cortical flash either before (more frequent) or after the main Ca^{2+} wave originates [16], the cortical flash in the eggs exposed to LAT-A invariably took place only after the intracellular Ca^{2+} wave had initiated. Hence, the cortical flash cannot be the priming cause of the Ca^{2+} wave in the eggs exposed to LAT-A. On the other hand, it is conceivable that the initial rise of the Ca^{2+} wave might have elicited cortical flash in a similar way whereby a Ca^{2+} wave driven by ionomycin or uncaged second messengers (e.g. $InsP_3$, cADPr, and NAADP) gives rise to ion influx and cortical flash in starfish eggs [16, 24, 51, 132]. Whereas the cADPr-elicited ion current in starfish oocytes was mainly through Na^+ channels, the train of action potentials that coincide with the cortical flash following LAT-A treatment required both Na^+ and Ca^{2+} in the extracellular space [71]. Hence, one model linking the two Ca^{2+} events in the eggs exposed to LAT-A (i.e. global Ca^{2+} wave and the short-lived cortical flash) might be that the enzyme PLCγ activated by F-actin disassembly produces $InsP_3$, and the resulting Ca^{2+}

increase evokes Ca^{2+} influx through voltage-gated Ca^{2+} channels. The latter event requires membrane depolarization, and might rely on opening of Na^{+} channels, which is known to be modulated either directly by Ca^{2+} or through calmodulin [133-136]. The model is compatible with the observation that the time lag between the first Ca^{2+} spot and cortical flash in the LAT-A-exposed egg is quite long (8 or up to 20 sec), but is not supported by the fact that cortical flash can be generated by LAT-A when no detectable Ca^{2+} wave is present, e.g. eggs preinjected with RFP-SH2 (Fig. 6). In this case, unless LAT-A renders the Ca^{2+}-induced Na^{+}/Ca^{2+} influx process extremely sensitive to the extent that it is operated by undetectable level of Ca^{2+} increase, F-actin disassembly might evoke cortical flash independently of the main Ca^{2+} wave by an unknown mechanism that requires as much time.

Our finding that depolymerization of suboolemmal actin filaments is sufficient for PLC activation and the generation of fertilization-like Ca^{2+} wave lets us rethink about the mechanism of egg activation by sperm. Fertilizing sperm induces drastic reorganization of suboolemmal actin cytoskeleton [47, 75]. In theory, our results suggest that extremely fast actin disassembly at the local site of sperm fusion could serve as an alternative way to generate Ca^{2+} wave and egg activation, but its demonstration may require a detection method of high time resolution. In essence, the phenomenon reported in this study is a parthenogenetic egg activation by an agent that changes the physical status of the suboolemmal actin cytoskeleton, and is reminiscent of sperm-free egg activation by proteases in marine worms, starfish, and other echinoderms [137]. As transmembrane proteins on the egg surface are thought to be mechanically linked to the subplasmalemmal actin cytoskeleton [138-141], which normally constrains the signaling molecules, it would be interesting to know how such events influence the suboolemmal cytoskeleton and effect Ca^{2+} increases and egg activation.

Acknowledgements

We thank Davide Caramiello for the management of the animals at MaReR of the *Stazione Zoologica Anton Dohrn*. We are also grateful to the staffs of DNA sequencing (SBM) and bioimaging services (AMOBIO) at the same institute for the technical assistance. We are also grateful to Dr. Alex McDougall (Sorbonne Universités, France) for kindly providing pET11-LifeAct-GFP. FV was partially supported by MIUR grant StarTregg, and NL by SZN PhD fellowship. This work was also supported by a Korean National Research Foundation Grant 2012R1A3A2026453 (to UHK).

Disclosure Statement

The authors declare no conflict of interests.

References

1 Brown DD: A tribute to the *Xenopus laevis* oocyte and egg. J Biol Chem 2004;279:45291-45299.
2 Hagiwara S, Jaffe LA: Electrical properties of egg cell membranes. Annu Rev Biophys Bioeng 1979;8:385-416.
3 Berridge MJ: Inositol trisphosphate and calcium signalling. Nature 1993;361:315-325.
4 Lee HC: Mechanisms of calcium signaling by cyclic ADP-ribose and NAADP. Physiol Rev 1997;77:1133-1164.
5 Santella L, Lim D, Moccia F: Calcium and fertilization: the beginning of life. Trends Biochem Sci 2004;29:400-408.
6 Whitaker M: Calcium at fertilization and in early development. Physiol Rev 2006;86:25-88.
7 Ridgway EB, Gilkey JC, Jaffe LF: Free calcium increases explosively in activating medaka eggs. Proc Natl Acad Sci U S A 1977;74:623-627.

8 Steinhardt R, Zucker R, Schatten G: Intracellular calcium release at fertilization in the sea urchin egg. Dev Biol 1977;58:185-196.
9 Jaffe LF: Classes and mechanisms of calcium waves. Cell Calcium 1993;14:736-745.
10 Miyazaki SI, Ohmori H, Sasaki S: Action potential and non-linear current-voltage relation in starfish oocytes. J Physiol 1975;246:37-54.
11 Miyazaki S: Thirty years of calcium signals at fertilization. Semin. Cell Dev Biol 2006;17:233-243.
12 Stricker SA: Comparative biology of calcium signaling during fertilization and egg activation in animals. Dev Biol 1999;211:157-176.
13 Santella L, Vasilev F, Chun JT: Fertilization in echinoderms. Biochem. Biophys Res Commun 2012;425:588-594.
14 Shen SS, Buck WR: Sources of calcium in sea urchin eggs during the fertilization response. Dev Biol 1993;157:157-169.
15 Churchill GC, O'Neill JS, Masgrau R, Patel S, Thomas JM, Genazzani AA, Galione A: Sperm deliver a new second messenger: NAADP. Curr Biol 2003;13:125-128.
16 Moccia F, Nusco GA, Lim D, Kyozuka K, Santella L: NAADP and $InsP_3$ play distinct roles at fertilization in starfish oocytes. Dev Biol 2006;294:24-38.
17 Whitaker MJ, Steinhardt RA: Ionic regulation of egg activation. Q Rev Biophys 1982;15:593-666.
18 Wessel GM, Brooks JM, Green E, Haley S, Voronina E, Wong J, Zaydfudim V, Conner S: The biology of cortical granules. Int Rev Cytol 2001;209:117-206.
19 Stack C, Lucero AJ, Shuster CB: Calcium-responsive contractility during fertilization in sea urchin eggs. Dev Dyn 2006;235:1042-1052.
20 Steinhardt RA, Epel D: Activation of sea-urchin eggs by a calcium ionophore. Proc Natl Acad Sci U S A 1974;71:1915-1919.
21 Carroll DJ, Albay DT, Hoang KM, O'Neill FJ, Kumano M, Foltz KR: The relationship between calcium, MAP kinase, and DNA synthesis in the sea urchin egg at fertilization. Dev Biol 2000;217:179-191.
22 Parrington J, Davis LC, Galione A, Wessel G: Flipping the switch: how a sperm activates the egg at fertilization. Dev Dyn 2007;236:2027-2038.
23 Galione A, White A, Willmott N, Turner M, Potter BV, Watson SP: cGMP mobilizes intracellular Ca^{2+} in sea urchin eggs by stimulating cyclic ADP-ribose synthesis. Nature 1993;365:456-459.
24 Nusco GA, Lim D, Sabala P, Santella L: Ca^{2+} response to cADPr during maturation and fertilization of starfish oocytes. Biochem Biophys Res Commun 2002;290:1015-1021.
25 Santella L, Nusco GA, Lim D: Calcium and Calcium-Linked Second Messengers are main Actors in the Maturation and Fertilization of Starfish Oocytes; in Lee HC (ed): Cyclic ADP-Ribose and NAADP: Structures, Metabolism and Functions. Boston, Keuwer Academic Publishers, 2002, pp. 381-396.
26 Santella L, Chun JT: Calcium Signaling by Cyclic ADP-Ribose and NAADP; in Lennarz WJ, Lane MD (eds): The Encyclopedia of Biological Chemistry. Waltham: Academic Press, 2013, Vol. 1, pp. 331-336.
27 Takahashi I, Kyozuka K: Development of Ca^{2+}-release mechanisms during oocyte maturation of the starfish *Asterina pectinifera*. Zygote 2016;24:857-868.
28 Runft LL, Jaffe LA, Mehlmann LM: Egg activation at fertilization: where it all begins. Dev Biol 2002;245:237-254.
29 Rhee SG: Regulation of phosphoinositide-specific phospholipase C. Annu Rev Biochem 2001;70:281-312.
30 Suh PG, Park JI, Manzoli L, Cocco L, Peak JC, Katan M, Fukami K, Kataoka T, Yun S, Ryu SH: Multiple roles of phosphoinositide-specific phospholipase C isozymes. BMB Rep 2008;41:415-434.
31 Saunders CM, Larman MG, Parrington J, Cox LJ, Royse J, Blayney LM, Swann K, Lai FA: PLC zeta: a sperm-specific trigger of Ca^{2+} oscillations in eggs and embryo development. Development 2002;129:3533-3544.
32 Hachem A, Godwin J, Ruas M, Lee HC, Ferrer Buitrago M, Ardestani G, Bassett A5, Fox S, Navarrete F, de Sutter P, Heindryckx B, Fissore R, Parrington J: PLCζ is the physiological trigger of the Ca^{2+} oscillations that induce embryogenesis in mammals but conception can occur in its absence. Development 2017;144:2914-2924.
33 Sea Urchin Genome Sequencing Consortium: The Genome of the Sea Urchin *Strongylocentrotus purpuratus.* Science 2006;314:941-952.

34 Hall MR, Kocot KM, Baughman KW, Fernandez-Valverde SL, Gauthier MEA, Hatleberg WL, Krishnan A, McDougall C, Motti CA, Shoguchi E, Wang T, Xiang X, Zhao M, Bose U, Shinzato C, Hisata K, Fujie M, Kanda M, Cummins SF, Satoh N, et al.: The crown-of-thorns starfish genome as a guide for biocontrol of this coral reef pest. Nature 2017;544:231-234.
35 Musacchia F, Vasilev F, Borra M, Biffali E, Sanges R, Santella L, Chun JT: *De novo* assembly of a transcriptome from the eggs and early embryos of *Astropecten aranciacus*. PLoS One 2017;12:e0184090.
36 Carroll DJ, Ramarao CS, Mehlmann LM, Roche S, Terasaki M, Jaffe LA: Calcium release at fertilization in starfish eggs is mediated by phospholipase Cgamma. J Cell Biol 1997;138:1303-1311.
37 Carroll DJ, Albay DT, Terasaki M, Jaffe LA, Foltz KR: Identification of PLCgamma-dependent and -independent events during fertilization of sea urchin eggs. Dev Biol 1999;206:232-247.
38 Runft LL, Carroll DJ, Gillett J, Giusti AF, O'Neill FJ, Foltz KR: Identification of a starfish egg PLC-gamma that regulates Ca^{2+} release at fertilization. Dev Biol 2004;269:220-236.
39 Giusti AF, Carroll DJ, Abassi YA, Foltz KR: Evidence that a starfish egg Src family tyrosine kinase associates with PLC-gamma1 SH2 domains at fertilization. Dev Biol 1999;208:189-199.
40 Abassi YA, Carroll DJ, Giusti AF, Belton RJ, Foltz KR: Evidence that Src-type tyrosine kinase activity is necessary for initiation of calcium release at fertilization in sea urchin eggs. Dev Biol 2000;218:206-219.
41 O'Neill FJ, Gillett J, Foltz KR: Distinct roles for multiple Src family kinases at fertilization. J Cell Sci 2004;117:6227-6238.
42 Turner PR, Jaffe LA, Fein A: Regulation of cortical vesicle exocytosis in sea urchin eggs by inositol 1, 4,5-trisphosphate and GTP-binding protein. J Cell Biol 1986;102:70-76.
43 Shilling FM, Carroll DJ, Muslin AJ, Escobedo JA, Williams LT, Jaffe LA: Evidence for both tyrosine kinase and G-protein-coupled pathways leading to starfish egg activation. Dev Biol 1994;162:590-599.
44 Kyozuka K, Chun JT, Puppo A, Gragnaniello G, Garante E, Santella L: Guanine nucleotides in the meiotic maturation of starfish oocytes: regulation of the actin cytoskeleton and of Ca^{2+} signaling. PLoS One 2009;4:e6296.
45 Just EE: The biology of the cell surface. Philadelphia. P. Blakiston's Son & co., Inc, 1939, pp. 75-103.
46 Lim D, Lange K, Santella L: Activation of oocytes by latrunculin A. FASEB J 2002;16:1050-1056.
47 Chun JT, Puppo A, Vasilev F, Gragnaniello G, Garante E, Santella L: The biphasic increase of PIP2 in the fertilized eggs of starfish: new roles in actin polymerization and Ca^{2+} signaling. PLoS One 2010;5:e14100.
48 Schroeder TE. Microfilament-mediated surface change in starfish oocytes in response to 1-methyladenine: implications for identifying the pathway and receptor sites for maturation-inducing hormones. J Cell Biol 1981;90:362-371.
49 Schroeder TE, Stricker SA: Morphological changes during maturation of starfish oocytes: surface ultrastructure and cortical actin. Dev Biol 1983;98:373-384.
50 Otto JJ, Schroeder TE: Assembly-disassembly of actin bundles in starfish oocytes: an analysis of actin-associated proteins in the isolated cortex. Dev Biol 1984;101:263-273.
51 Vasilev F, Chun JT, Gragnaniello G, Garante E, Santella L: Effects of ionomycin on egg activation and early development in starfish. PLoS One 2012;7:e39231.
52 Dale B, de Santis A, Hoshi M: Membrane response to 1-methyladenine requires the presence of the nucleus. Nature 1979;282:89-90.
53 Moody WJ, Bosma MM: Hormone-induced loss of surface membrane during maturation of starfish oocytes: differential effects on potassium and calcium channels. Dev Biol 1985;112:396-404.
54 Santella L, Limatola N, Chun JT: Calcium and actin in the saga of awakening oocytes. Biochem Biophys Res Commun 2015;460:104-113.
55 Terasaki M: Redistribution of cytoplasmic components during germinal vesicle breakdown in starfish oocytes. J Cell Sci 1994;107:1797-1805.
56 Chiba K, Kado RT, Jaffe LA: Development of calcium release mechanisms during starfish oocyte maturation. Dev Biol 1990;140:300-306.
57 Lim D, Ercolano E, Kyozuka K, Nusco GA, Moccia F, Lange K, Santella L: The M-phase-promoting factor modulates the sensitivity of the Ca^{2+} stores to inositol 1, 4,5-trisphosphate via the actin cytoskeleton. J Biol Chem 2003;278:42505-42514.
58 Janmey PA: The cytoskeleton and cell signaling: component localization and mechanical coupling. Physiol Rev 1998;78:763-781.

59 Sheng M, Pak DT: Ligand-gated ion channel interactions with cytoskeletal and signaling proteins. Annu Rev Physiol 2000;62:755-778.
60 Calaghan SC, Le Guennec JY, White E: Cytoskeletal modulation of electrical and mechanical activity in cardiac myocytes. Prog. Biophys. Mol Biol 2004;84:29-59.
61 Dalghi MG, Ferreira-Gomes M, Rossi JP: Regulation of the Plasma Membrane Calcium ATPases by the actin cytoskeleton. Biochem Biophys Res Commun DOI: 10.1016/j.bbrc.2017.11.151.
62 Nusco GA, Chun JT, Ercolano E, Lim D, Gragnaniello G, Kyozuka K, Santella L: Modulation of calcium signalling by the actin-binding protein cofilin. Biochem Biophys Res Commun 2006;348:109-114.
63 Chun JT, Vasilev F, Santella L: Antibody against the actin-binding protein depactin attenuates Ca^{2+} signaling in starfish eggs. Biochem. Biophys Res Commun 2013;441:301-307.
64 Chun JT, Limatola N, Vasilev F, Santella L: Early events of fertilization in sea urchin eggs are sensitive to actin-binding organic molecules. Biochem Biophys Res Commun 2014;450:1166-1174.
65 Kyozuka K, Chun JT, Puppo A, Gragnaniello G, Garante E, Santella L: Actin cytoskeleton modulates calcium signaling during maturation of starfish oocytes. Dev Biol 2008;320:426-435.
66 Limatola N, Chun JT, Kyozuka K, Santella L: Novel Ca^{2+} increases in the maturing oocytes of starfish during the germinal vesicle breakdown. Cell Calcium 2015;58:500-510.
67 Lange K, Gartzke J: F-actin-based Ca signaling-a critical comparison with the current concept of Ca signaling. J Cell Physiol 2006;209:270-287.
68 Chun JT, Santella L: The actin cytoskeleton in meiotic maturation and fertilization of starfish eggs. Biochem Biophys Res Commun 2009;384:141-143.
69 Coué M, Brenner SL, Spector I, Korn ED: Inhibition of actin polymerization by latrunculin A. FEBS Lett 1987;213:316-318.
70 Yarmola EG, Somasundaram T, Boring TA, Spector I, Bubb MR: Actin-latrunculin A structure and function. Differential modulation of actin-binding protein function by latrunculin A J Biol Chem 2000;275:28120-28127.
71 Moccia F: Latrunculin A depolarizes starfish oocytes. Comp Biochem Physiol A Mol Integr Physiol 2007;148: 845-852.
72 Hill TD, Berggren PO, Boynton AL: Heparin inhibits inositol trisphosphate-induced calcium release from permeabilized rat liver cells. Biochem Biophys Res Commun 1987;149:897-901.
73 Nilsson T, Zwiller J, Boynton AL, Berggren PO: Heparin inhibits IP3-induced Ca^{2+} release in permeabilized pancreatic beta-cells. FEBS Lett 1988;229:211-214.
74 Cullen PJ, Comerford JG, Dawson AP: Heparin inhibits the inositol 1, 4,5-trisphosphate-induced Ca^{2+} release from rat liver microsomes. FEBS Lett 1988;228:57-59.
75 Puppo A, Chun JT, Gragnaniello G, Garante E, Santella L: Alteration of the cortical actin cytoskeleton deregulates Ca^{2+} signaling, monospermic fertilization, and sperm entry. PLoS One 2008;3:e3588.
76 Gokina NI, Osol G: Actin cytoskeletal modulation of pressure-induced depolarization and Ca^{2+} influx in cerebral arteries. Am J Physiol Heart Circ Physiol 2002;282:H1410-1420.
77 Fujimoto T, Miyawaki A, Mikoshiba K: Inositol 1, 4,5-trisphosphate receptor-like protein in plasmalemmal caveolae is linked to actin filaments. J Cell Sci 1995;108:7-15.
78 Fukatsu K, Bannai H, Zhang S, Nakamura H, Inoue T, Mikoshiba K: Lateral diffusion of inositol 1, 4,5-trisphosphate receptor type 1 is regulated by actin filaments and 4.1N in neuronal dendrites. J Biol Chem 2004;279:48976-48982.
79 Jaffe LA, Terasaki M: Structural changes in the endoplasmic reticulum of starfish oocytes during meiotic maturation and fertilization. Dev Biol 1994;164:579-587.
80 Schacht J: Purification of polyphosphoinositides by chromatography on immobilized neomycin. J Lipid Res 1978;19:1063-1067.
81 Arbuzova A, Martushova K, Hangyás-Mihályné G, Morris, Ozaki S, Prestwich GD, McLaughlin S: Fluorescently labeled neomycin as a probe of phosphatidylinositol-4, 5-bisphosphate in membranes. Biochim Biophys Acta 2000;1464:35-1448.
82 Swann K, Whitaker M: The part played by inositol trisphosphate and calcium in the propagation of the fertilization wave in sea urchin eggs. J Cell Biol 1986;103:2333-2242.
83 Gabev E, Kasianowicz J, Abbott T, McLaughlin S: Binding of neomycin to phosphatidylinositol 4, 5-bisphosphate (PIP2). Biochim Biophys Acta 1989;979:105-112.

84 Hammond GR, Dove SK, Nicol A, Pinxteren JA, Zicha D, Schiavo G: Elimination of plasma membrane phosphatidylinositol (4, 5)-bisphosphate is required for exocytosis from mast cells. J Cell Sci 2006;119:2084-2094.
85 Liscovitch M, Chalifa V, Danin M, Eli Y: Inhibition of neural phospholipase D activity by aminoglycoside antibiotics. Biochem J 1991;279:319-321.
86 Smith RJ, Sam LM, Justen JM, Bundy GL, Bala GA, Bleasdale JE: Receptor-coupled signal transduction in human polymorphonuclear neutrophils: effects of a novel inhibitor of phospholipase C-dependent processes on cell responsiveness. J Pharmacol Exp Ther 1990;253:688-697.
87 Bleasdale JE, Thakur NR, Gremban RS, Bundy GL, Fitzpatrick FA, Smith RJ, Bunting S: Selective inhibition of receptor-coupled phospholipase C-dependent processes in human platelets and polymorphonuclear neutrophils. J Pharmacol Exp Ther 1990;255:756-768.
88 Berven LA, Barritt GJ: Evidence obtained using single hepatocytes for inhibition by the phospholipase C inhibitor U73122 of store-operated Ca^{2+} inflow. Biochem Pharmacol 1995;49:1373-1379.
89 Macmillan, D. and J.G. McCarron: The phospholipase C inhibitor U-73122 inhibits Ca^{2+} release from the intracellular sarcoplasmic reticulum Ca^{2+} store by inhibiting Ca^{2+} pumps in smooth muscle. Br J Pharmacol 2010;160:1295-1301.
90 Leitner MG, Michel N, Behrendt M, Dierich M, Dembla S, Wilke BU, Konrad M, Lindner M, Oberwinkler J, Oliver D: Direct modulation of TRPM4 and TRPM3 channels by the phospholipase C inhibitor U73122. Br J Pharmacol 2016;173:2555-2569.
91 Matsui S, Adachi R, Kusui K, Yamaguchi T, Kasahara T, Hayakawa T, Suzuki K: U73122 inhibits the dephosphorylation and translocation of cofilin in activated macrophage-like U937 cells. Cell Signal 2001;13:17-22.
92 Saul D, Fabian L, Forer A, Brill JA: Continuous phosphatidylinositol metabolism is required for cleavage of crane fly spermatocytes. J Cell Sci 2004;117:3887-3896.
93 Yagisawa H, Hirata M, Kanematsu T, Watanabe Y, Ozaki S, Sakuma K, Tanaka H, Yabuta N, Kamata H, Hirata H: Expression and characterization of an inositol 1, 4,5-trisphosphate binding domain of phosphatidylinositol-specific phospholipase C-δ1. J Biol Chem 1994;269:20179-20188.
94 Stauffer TP, Ahn S, Meyer T: Receptor-induced transient reduction in plasma membrane PtdIns(4, 5)P2 concentration monitored in living cells. Curr Biol 1998;8:343-346.
95 Várnai P, Balla T: Visualization of phosphoinositides that bind pleckstrin homology domains: calcium- and agonist-induced dynamic changes and relationship to myo-[^{3}H]inositol-labeled phosphoinositide pools. J Cell Biol 1998;143:501-510.
96 Watt SA, Kular G, Fleming IN, Downes CP, Lucocq JM: Subcellular localization of phosphatidylinositol 4, 5-bisphosphate using the pleckstrin homology domain of phospholipase C δ1. Biochem J 2002;363:657–666.
97 Lemmon MA, Ferguson KM, O'Brien R, Sigler PB, Schlessinger J: Specific and high-affinity binding of inositol phosphates to an isolated pleckstrin homology domain. Proc Natl Acad Sci U S A 1995;92:10472-10476.
98 Hirose K, Kadowaki S, Tanabe M, Takeshima H, Iino M: Spatiotemporal dynamics of inositol 1, 4,5-trisphosphate that underlies complex Ca^{2+} mobilization patterns. Science 1999;284:1527-1530.
99 Xu C, Watras J, Loew LM: Kinetic analysis of receptor-activated phosphoinositide turnover. J Cell Biol 2003;161:779–791.
100 Carafoli E, Santella L, Branca D, Brini M: Generation, control, and processing of cellular calcium signals. Crit Rev Biochem Mol Biol 2001;36:107-260.
101 Rosales C, Jones SL, McCourt D, Brown EJ: Bromophenacyl bromide binding to the actin-bundling protein l-plastin inhibits inositol trisphosphate-independent increase in Ca^{2+} in human neutrophils. Proc Natl Acad Sci U S A 1994;91:3534-3548.
102 Arrieumerlou C, Randriamampita C, Bismuth G, Trautmann A: Rac is involved in early TCR signaling. J Immunol 2000;165:3182-3189.
103 Diamond SL, Sachs F, Sigurdson WJ: Mechanically induced calcium mobilization in cultured endothelial cells is dependent on actin and phospholipase. Arterioscler Thromb 1994;14:2000-2006.
104 Béliveau E, Guillemette G: Microfilament and microtubule assembly is required for the propagation of inositol trisphosphate receptor-induced Ca^{2+} waves in bovine aortic endothelial cells. J Cell Biochem 2009;106:344-352.

105 Frigeri L, Apgar JR: The role of actin microfilaments in the down-regulation of the degranulation response in RBL-2H3 mast cells. J Immunol 1999;162:2243-2250.
106 Geeraert V, Dupont JL, Grant NJ, Huvet C, Chasserot-Golaz S, Janoshazi A, Procksch O, de Barry J: F-actin does not modulate the initial steps of the protein kinase C activation process in living nerve cells. Exp Cell Res 2003;289:222-236.
107 Schubert T, Akopian A: Actin filaments regulate voltage-gated ion channels in salamander retinal ganglion cells. Neuroscience 2004;125:583-590.
108 Houssen WE, Jaspars M, Wease KN, Scott RH: Acute actions of marine toxin latrunculin A on the electrophysiological properties of cultured dorsal root ganglion neurones. Comp Biochem Physiol C Toxicol Pharmacol 2006;142:19-29.
109 Santella L, Kyozuka K: Reinitiation of meiosis in starfish oocytes requires an increase in nuclear Ca^{2+}. Biochem Biophys Res Commun 1994;203:674-680.
110 Oka T, Sato K, Hori M, Ozaki H, Karaki H: FcεRI cross-linking-induced actin assembly mediates calcium signalling in RBL-2H3 mast cells. Br J Pharmacol 2002;136:837-846.
111 Horstman DA, Takemura H, Putney JW: Formation and metabolism of [^{3}H]inositol phosphates in AR42J pancreatoma cells. Substance P-induced Ca^{2+} mobilization in the apparent absence of inositol 1, 4,5-trisphosphate 3-kinase activity. J Biol Chem 1988;263:15297-152303.
112 Kisihgami A, Ogasawara T, Watanabe Y, Hirata M, Maeda T, Hayashi F, Tsukahara Y: Inositol-1, 4,5-trisphosphate-binding proteins controlling the phototransduction cascade of invertebrate visual cells. J Exp Biol 2001;204:487-493.
113 Guse AH: Linking NAADP to ion channel activity: a unifying hypothesis. Sci Signal 2012;5:pe18.
114 Yu JC, Lloyd-Burton SM, Irvine RF, Schell MJ: Regulation of the localization and activity of inositol 1, 4,5-trisphosphate 3-kinase B in intact cells by proteolysis. Biochem J 2005;392:435-441.
115 Shawl AI, Park KH, Kim BJ, Higashida C, Higashida H, Kim UH: Involvement of actin filament in the generation of Ca^{2+} mobilizing messengers in glucose-induced Ca^{2+} signaling in pancreatic β-cells. Islets 2012;4:145-151.
116 Lange K: Microvillar Ca^{++} signaling: a new view of an old problem. J Cell Physiol 1999;180:19-34.
117 Baeker TR, Simons ER, Rothstein TL: Cytochalasin induces an increase in cytosolic free calcium in murine B lymphocytes. J Immunol 1987;138:2691-2697.
118 van Haelst C, Rothstein TL: Cytochalasin stimulates phosphoinositide metabolism in murine B lymphocytes. J Immunol 1988;140:1256-1258.
119 Polliack A: The contribution of scanning electron microscopy in haematology: its role in defining leucocyte and erythrocyte disorders. J Microsc 1981;123:177-187.
120 Majstoravich S, Zhang J, Nicholson-Dykstra S, Linder S, Friedrich W, Siminovitch KA, Higgs HN: Lymphocyte microvilli are dynamic, actin-dependent structures that do not require Wiskott-Aldrich syndrome protein (WASp) for their morphology. Blood 2004;104:1396-1403.
121 Grondin P, Plantavid M, Sultan C, Breton M, Mauco G, Chap H: Interaction of pp60c-src, phospholipase C, inositol-lipid, and diacyglycerol kinases with the cytoskeletons of thrombin-stimulated platelets. J Biol Chem 1991;266:15705-15709.
122 Baldassare JJ, Henderson PA, Tarver A, Fisher GJ: Thrombin activation of human platelets dissociates a complex containing gelsolin and actin from phosphatidylinositide-specific phospholipase Cgamma1. Biochem J 1997;324:283-287.
123 McBride K, Rhee SG, Jaken S: Immunocytochemical localization of phospholipase C-gamma in rat embryo fibroblasts. Proc Natl Acad Sci U S A 1991;88:7111-7115.
124 Yang LJ, Rhee SG, Williamson JR: Epidermal growth factor-induced activation and translocation of phospholipase C-gamma 1 to the cytoskeleton in rat hepatocytes. J Biol Chem 1994;269:7156-7162.
125 Dearden-Badet MT, Mouchiroud G: Re-distribution of phospholipase C gamma 2 in macrophage precursors is mediated by the actin cytoskeleton under the control of the Src kinases. Cell Signal 2005;17:1560-1571.
126 Huang CH, Crain RC: Phosphoinositide-specific phospholipase C in oat roots: association with the actin cytoskeleton. Planta 2009;230:925-933.
127 Helmke S, Pfenninger KH: Growth cone enrichment and cytoskeletal association of non-receptor tyrosine kinases. Cell Motil Cytoskeleton 1995;30:194-207.
128 Pei Z, Yang L, Williamson JR: Phospholipase C-gamma 1 binds to actin-cytoskeleton via its C-terminal SH2 domain *in vitro*. Biochem Biophys Res Commun 1996;228:802-806.

129 Gresset A, Hicks SN, Harden TK, Sondek J: Mechanism of phosphorylation-induced activation of phospholipase C-gamma isozymes. J Biol Chem 2010;285:35836-35847.
130 Lassing I, Lindberg U: Specific interaction between phosphatidylinositol 4, 5-bisphosphate and profilactin. Nature 1985;314:472-474.
131 Forscher P: Calcium and polyphosphoinositide control of cytoskeletal dynamics. Trends Neurosci 1989;12:468-474.
132 Moccia F, Nusco GA, Lim D, Ercolano E, Gragnaniello G, Brown ER, Santella L: Ca^{2+} signalling and membrane current activated by cADPr in starfish oocytes. Pflugers Arch 2003;446:541-552.
133 Babitch J: Channel hands. Nature 1990;346:321-322.
134 Shah VN, Wingo TL, Weiss KL, Williams CK, Balser JR, Chazin WJ: Calcium-dependent regulation of the voltage-gated sodium channel hH1: intrinsic and extrinsic sensors use a common molecular switch. Proc Natl Acad Sci U S A 2006;103:3592-3597.
135 Aiba T, Hesketh GG, Liu T, Carlisle R, Villa-Abrille MC, O'Rourke B, Akar FG, Tomaselli GF: Na^+ channel regulation by Ca^{2+}/calmodulin and Ca^{2+}/calmodulin-dependent protein kinase II in guinea-pig ventricular myocytes. Cardiovasc Res 2010;85:454-463.
136 Pitt GS, Lee SY: Current view on regulation of voltage-gated sodium channels by calcium and auxiliary proteins. Protein Sci 2016;25:1573-1584.
137 Carroll DJ, Jaffe LA: Proteases stimulate fertilization-like responses in starfish eggs. Dev Biol 1995;170:690-700.
138 Ingber D: Integrins as mechanochemical transducers. Curr Opin Cell Biol 1991;3:841-848.
139 Ingber DE: Tensegrity: the architectural basis of cellular mechanotransduction. Annu Rev Physiol 1997;59:575-599.
140 Davies E: Intercellular and intracellular signals and their transduction via the plasma membrane-cytoskeleton interface. Semin Cell Biol 1993;4:139-147.
141 Maniotis AJ, Chen CS, Ingber DE: Demonstration of mechanical connections between integrins, cytoskeletal filaments, and nucleoplasm that stabilize nuclear structure. Proc Natl Acad Sci U S A 1997;94:849-854.